

Three R2R3-MYB Transcription Factors Regulate Distinct Floral Pigmentation Patterning in *Phalaenopsis* spp.¹[OPEN]

Chia-Chi Hsu, You-Yi Chen, Wen-Chieh Tsai, Wen-Huei Chen, and Hong-Hwa Chen*

Department of Life Sciences (C.-C.H., Y.-Y.C., H.-H.C.), Institute of Tropical Plant Sciences (W.-C.T.), and Orchid Research and Development Center (W.-C.T., W.-H.C., H.-H.C.), National Cheng Kung University, Tainan 701, Taiwan

Orchidaceae are well known for their fascinating floral morphologic features, specialized pollination, and distinctive ecological strategies. With their long-lasting flowers of various colors and pigmentation patterning, *Phalaenopsis* spp. have become important ornamental plants worldwide. In this study, we identified three R2R3-MYB transcription factors *PeMYB2*, *PeMYB11*, and *PeMYB12*. Their expression profiles were concomitant with red color formation in *Phalaenopsis* spp. flowers. Transient assay of overexpression of three *PeMYBs* verified that *PeMYB2* resulted in anthocyanin accumulation, and these *PeMYBs* could activate the expression of three downstream structural genes *Phalaenopsis* spp. *Flavanone 3-hydroxylase5*, *Phalaenopsis* spp. *Dihydroflavonol 4-reductase1*, and *Phalaenopsis* spp. *Anthocyanidin synthase3*. In addition, these three *PeMYBs* participated in the distinct pigmentation patterning in a single flower, which was revealed by virus-induced gene silencing. In the sepals/petals, silencing of *PeMYB2*, *PeMYB11*, and *PeMYB12* resulted in the loss of the full-red pigmentation, red spots, and venation patterns, respectively. Moreover, different pigmentation patterning was regulated by *PeMYBs* in the sepals/petals and lip. *PeMYB11* was responsive to the red spots in the callus of the lip, and *PeMYB12* participated in the full pigmentation in the central lobe of the lip. The differential pigmentation patterning was validated by RNA in situ hybridization. Additional assessment was performed in six *Phalaenopsis* spp. cultivars with different color patterns. The combined expression of these three *PeMYBs* in different ratios leads to a wealth of complicated floral pigmentation patterning in *Phalaenopsis* spp.

Phalaenopsis spp., one genus of Orchidaceae, have become very popular worldwide for their long-lived flowers with various colors and pigmentation patterns. In addition to the two lateral petals, the third petal is modified into a labellum or lip to attract pollinators. Their flower colors range from black to purple, red, yellow, and white, and differential coloration generates various pigmentation patterns, such as spots, irregular blotches, stripes overlaying veins (venation pattern), or combinations of these (Supplemental Fig. S1). Pigmentation patterning may increase successful pollination by both increasing the frequency of pollinator visits and providing color guides for the location of rewards, pollen, and nectar or preferred landing platforms of the flower (Medel et al., 2003; Heuschen et al., 2005; Lunau et al., 2006; Ushimaru et al., 2007). Of note, both the color and the pigmentation patterning usually differ between the sepals/petals and the lip of a *Phalaenopsis* spp. flower. This observation indicates a distinct regulatory mechanism within a single *Phalaenopsis* spp. flower for the accumulation of anthocyanins, the water-soluble pigments occurring in almost all plants that are responsible

for most of the orange, red, purple, and blue colors of flowers. With all of the above-mentioned characteristics, *Phalaenopsis* spp. with natural variations in flower colors would be an excellent model plant for studying the molecular mechanism regulating floral pigmentation patterning.

The biosynthetic pathway for anthocyanins is one of the most extensively studied plant secondary metabolisms (Grotewold, 2006). Many regulatory genes involved in the anthocyanin biosynthetic pathway have been cloned and characterized from a wide variety of plants. R2R3-MYB, basic helix-loop-helix (bHLH) transcription factors, and WD40 repeat (WDR) proteins are the three major families of regulatory proteins for anthocyanin biosynthesis (Koes et al., 2005; Feller et al., 2011; Hichri et al., 2011; Petroni and Tonelli, 2011).

The R2R3-MYB transcription factors play a major role in determining the spatial and temporal patterning of anthocyanins in *Antirrhinum* spp. and *Petunia* spp. (Schwinn et al., 2006; Albert et al., 2011; Davies et al., 2012). Irregular pigmentation patterning, such as color flecks and sectors, was studied in morning glory (*Pharbitis purpurea*) and other plants and found to be linked to the activated transposon insertion in anthocyanin biosynthetic genes (Inagaki et al., 1994; Iida et al., 1999; Itoh et al., 2002). Other patterns, such as in *Petunia* spp. Red Star and *Petunia* spp. picotee, flowers are the result of reduced RNA expression of *Chalcone synthase* (*CHS*), possibly because of short-interfering RNA degradation (Koseki et al., 2005; Saito et al., 2006; Griesbach et al., 2007). The spot pattern is associated with the differential expression of *Dihydroflavonol 4-reductase2* (*Dfr2*) in the

¹ This work was supported by the Ministry of Science and Technology, Taiwan (grant no. NSC 103-2321-B-006-002).

* Address correspondence to hhchen@mail.ncku.edu.tw.

The author responsible for distribution of materials integral to the findings presented in this article in accordance with the policy described in the Instructions for Authors (www.plantphysiol.org) is: Hong-Hwa Chen (hhchen@mail.ncku.edu.tw).

[OPEN] Articles can be viewed without a subscription.

www.plantphysiol.org/cgi/doi/10.1104/pp.114.254599

red-purple spot in *Clarkia gracilis* (Martins et al., 2013) or light-induced *Lilium hybrid MYB6* (*LhMYB6*) in the red spots compared with the pink background regulated by *LhMYB12* in the Asiatic hybrid lily (*Lilium* spp.) 'Montreux' (Yamagishi et al., 2010). Splatter-type spots in the Asiatic hybrid lily 'Latvia' are regulated by a unique allele of *LhMYB12-Lat* (Yamagishi et al., 2014). Moreover, the anthocyanin phenotypes of leaf blotching, calyx spotting, and corolla banding were varied within the populations of *Mimulus guttatus* and controlled by *Petal Lobe Anthocyanin1* locus, which contains three tandem repeats of R2R3-MYB genes (Lowry et al., 2012). However, the genetic control of petal spots has not been well studied and may differ among species.

In Orchidaceae, *Phalaenopsis schilleriana DFR* (*PsDFR*) and *PsMYB* express in the purple flowers of *P. schilleriana* and spots of *Phalaenopsis* spp. 'Ever-spring Fairy' petals but not in white-flower *Phalaenopsis amabilis* (Ma et al., 2009). In *Oncidium* spp. 'Gower Ramsey,' the expression of *Oncidium gower Chalcone isomerase* (*OgCHI*), *OgDFR*, and *OgMYB1* confers a lip crest with a mosaic red pigmentation in flowers (Chiou and Yeh, 2008).

Virus-induced gene silencing (VIGS) is a reverse genetics approach used for functional analysis of genes in plants, especially those with long lifecycles and few genetic resources, such as *Phalaenopsis* spp. A *Cymbidium* mosaic virus (CymMV)-based VIGS vector and its modified vector have been established (Lu et al., 2007, 2012) and were used to determine the effect of *Phalaenopsis* spp. *TF15* (*PhaTF15*) on disease resistance (Lu et al., 2012), *Phalaenopsis equestris* UDP glucose: flavonoid 3-O-glucosyltransferase (*PeUFGT3*) on anthocyanin biosynthesis (Chen et al., 2011), *P. equestris* *MADS5* (*PeMADS5*), *PeMADS6*, *P. equestris* *SEPALLATA1* (*PeSEP1*), *PeSEP2*, *PeSEP3*, and *PeSEP4* on floral morphogenesis (Hsieh et al., 2013a; Pan et al., 2014), and high-throughput silencing of 126 transcription factors for identifying genes involved in flower development of *Phalaenopsis* spp. (Hsieh et al., 2013b).

In this study, we identified three R2R3-MYB transcription factors (*PeMYB2*, *PeMYB11*, and *PeMYB12*) in *Phalaenopsis* spp. and analyzed their expression profiles. We used transient assay of gene overexpression to verify that these three *PeMYBs* can activate the expression of the downstream structural genes and result in anthocyanin accumulation. Moreover, these three *PeMYBs* individually participated in regulating the distinct pigmentation patterning in *Phalaenopsis* spp., which was revealed by VIGS and RNA in situ hybridization. The expression of the three *PeMYBs* and their mutual interaction were confirmed in various *Phalaenopsis* spp. cultivars.

RESULTS

Phylogenetic Relationships of R2R3-MYB Transcription Factors Isolated from *Phalaenopsis* spp.

To study the MYB transcription factors that regulate anthocyanin biosynthesis in *Phalaenopsis* spp., we identified 16 R2R3-MYB transcription factors (*PeMYB1–PeMYB16*), including 14 *PeMYBs* isolated from OrchidBase (Fu et al.,

2011; Tsai et al., 2013) and 2 *PeMYBs* amplified from *P. equestris* with degenerated primers. Phylogenetic analysis showed *PeMYB2*, *PeMYB11*, and *PeMYB12* in the same clade as *Zea mays* C1 (*ZmC1*), which controls the pigmentation of seeds or kernels (Paz-Ares et al., 1987; Lepiniec et al., 2006), and the same large cluster with dicot anthocyanin-promoting MYBs, including *Petunia hybrida* Anthocyanin2 (*PhAN2*) and *Antirrhinum majus* VENOSA (*AmVENOSA*), *AmROSEA1* (*AmROS1*), and *AmROS2* (Fig. 1). *PeMYB11* was most similar to purple-flower orchid *PsMYB* (Ma et al., 2009) and *Oncidium* spp. *OgMYB1* in regulating red color formation (Chiou and Yeh, 2008; Fig. 1). *PeMYB1*, *PeMYB13*, and *PeMYB14* were grouped together, and *PeMYB3* was in another clade with *Z. mays* P (*ZmP*; Fig. 1). Otherwise, *PeMYB4*, *PeMYB5*, *PeMYB6*, *PeMYB7*, and *PeMYB8* were grouped with *AtMYB4* (Jin et al., 2000), *Fragaria ananassa* MYB1 (*FaMYB1*; Aharoni et al., 2001), and other MYBs that are repressors of flavonoid biosynthesis (Fig. 1).

Multiple alignment of the MYB-R2R3 region showed that the sequences of *PeMYB2*, *PeMYB11*, and *PeMYB12* contained a conserved [D/E]Lx₂[R/K]x₃Lx₆Lx₃R motif at positions 65 to 84 required for interaction with R/B-like bHLH proteins (Zimmermann et al., 2004; Fig. 2, arrows). However, they lack the three conserved amino acid residues (R39, V64, and A90), and a convenient identifier, ANDV, at positions 90 to 93 of dicot anthocyanin-promoting MYBs (Lin-Wang et al., 2010; Fig. 2, arrowheads).

Expression of *PeMYB2*, *PeMYB11*, and *PeMYB12* Was Concomitant with Red Color Formation in Flowers

The expression profiles of the *PeMYBs* were first assessed in *Phalaenopsis aphrodite* ssp. *formosana* with white sepals/petals and a yellow lip (Fig. 3A) and *Phalaenopsis* spp. OX Brother Seamate 'OX1313' with white sepals/petals and a red lip (Fig. 3B) by reverse transcription (RT)-PCR (Supplemental Fig. S2F). In *P. aphrodite* ssp. *formosana*, transcripts of *PeMYB2* and *PeMYB11* were detected in the sepals and lip, respectively (Supplemental Fig. S2F), concomitant with the pink color formation on the abaxial surface of the sepals (Supplemental Fig. S2C) and the red spots on the callus and lateral lobes of the lip (Supplemental Fig. S2B), respectively. In *Phalaenopsis* spp. OX Brother Seamate 'OX1313,' the expression of *PeMYB11* and *PeMYB12* was detected in the red lip (Supplemental Fig. S2F), but *PeMYB2* expressed in the sepals and petals, which was concomitant with the pink color on the abaxial surfaces of both sepals and petals (Supplemental Fig. S2, D and E). In contrast, *PeMYB3*, *PeMYB4*, *PeMYB5*, *PeMYB7*, *PeMYB8*, and *PeMYB16* expressed in all three floral organs at different levels (Supplemental Fig. S2F), with little or no expression of *PeMYB1*, *PeMYB6*, *PeMYB9*, *PeMYB10*, and *PeMYB13* to *PeMYB15* in these floral organs (Supplemental Fig. S2F).

The expression profiles of *PeMYB2*, *PeMYB11*, and *PeMYB12* were further assessed in *P. aphrodite* ssp.

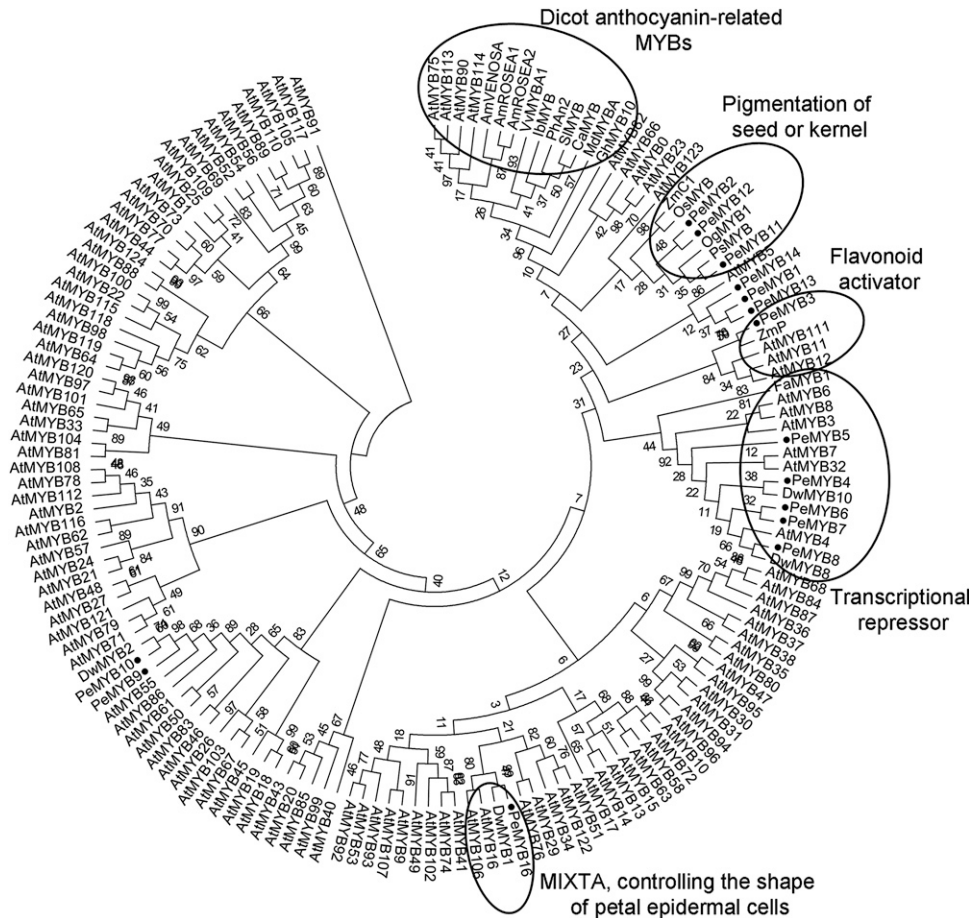


Figure 1. Phylogenetic tree inferred from the amino acid sequences of the R2R3 region of PeMYBs with anthocyanin-related MYBs and all *Arabidopsis thaliana* R2R3-MYBs. This phylogenetic tree was constructed by the Maximum Likelihood method with 1,000 bootstrapping data sets. Black circles indicate 15 PeMYBs identified in this study. MIXTA is an R2R3-MYB gene in *A. majus* and controls the development of conical cell shape in petal epidermal cells (Baumann et al., 2007).

formosana and *Phalaenopsis* spp. OX Brother Seamate 'OX1313' and compared with the red-flower *Phalaenopsis* spp. OX Red Shoe 'OX1408' by quantitative real-time reverse transcription (qRT)-PCR (Fig. 3). Little or no expression of *PeMYB2* and *PeMYB12* was detected in any of the floral organs of the white-flower *P. aphrodite* ssp. *formosana*, with *PeMYB11* slightly expressed in the lip (Fig. 3, A, D, and E), which was associated with the red spots in the callus and lateral lobes of the lip (Supplemental Fig. S2B). For white-flower/red-lip *Phalaenopsis* spp. OX Brother Seamate 'OX1313,' the expression of *PeMYB12* was higher than that of both *PeMYB2* and *PeMYB11* in the lip (Fig. 3, D and E), and low-level expression of *PeMYB2* and *PeMYB12* in the sepals and petals was associated with the pink color on abaxial surfaces (Fig. 3, D and E; Supplemental Fig. S2, D and E). *PeMYB2*, *PeMYB11*, and *PeMYB12* were highly expressed in the floral organs of the red-flower *Phalaenopsis* spp. OX Red Shoe 'OX1408,' except that *PeMYB2* showed lower expression in the lip (Fig. 3, C-E). Thus, the differential expression of *PeMYB2*, *PeMYB11*, and *PeMYB12* was concomitant with the red color formation in these three *Phalaenopsis* spp. with different flower colors, which indicates that they are involved in the regulation of the anthocyanin biosynthesis in *Phalaenopsis* spp.

Expression of *PebHLH1*, *PebHLH2*, *PebHLH3*, and *PeWDR1* Was Not Concomitant with the Red Color Formation

R2R3-MYB transcription factors are known to form complexes with bHLH and WDR factors to regulate anthocyanin biosynthesis. We identified three bHLH transcription factors and one WDR protein from OrchidBase. *PebHLH1* was grouped with PhAN1 (Spelt et al., 2000), and *PebHLH2* and *PebHLH3* were categorized with *Z. mays* Leaf color (*ZmLc*; Ludwig et al., 1989) and *A. majus* DELILA (Goodrich et al., 1992; Supplemental Fig. S3). Real-time RT-PCR results showed that, in white-flower *P. aphrodite* ssp. *formosana*, high expression of *PebHLH3* was only detected in the lip, whereas *PebHLH1* and *PebHLH2* expressed slightly in the sepals, petals, and lip (Supplemental Fig. S4). For white-flower/red-lip *Phalaenopsis* spp. OX Brother Seamate 'OX1313,' no differential expression of *PebHLH2* and *PebHLH3* was detected in these three floral organs, whereas *PebHLH1* expressed higher in sepal than petal and lip (Supplemental Fig. S4). In the red-flower *Phalaenopsis* spp. OX Red Shoe 'OX1408,' *PebHLH3* was highly expressed in all three floral organs, whereas *PebHLH2* expressed similarly in these three floral organs (Supplemental Fig. S4). The expression pattern of *PebHLH1* was similar in *Phalaenopsis* spp. OX Brother

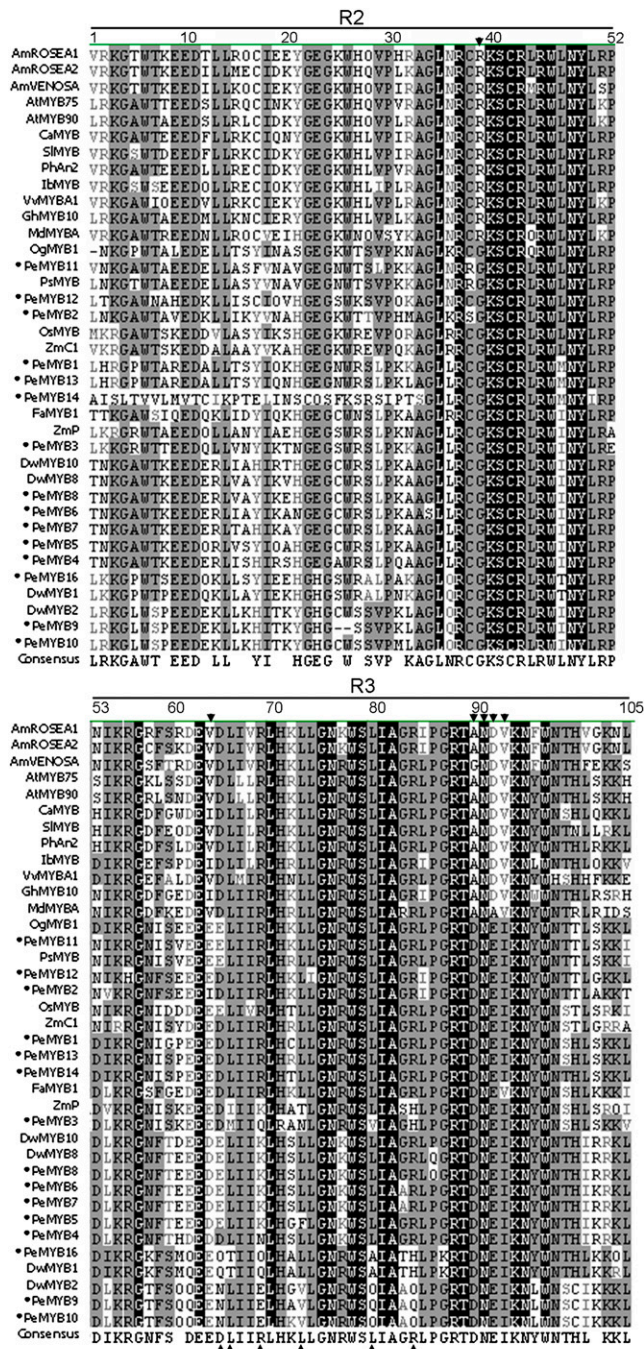


Figure 2. Multiple alignment of the amino acid sequences in the R2R3 region of PeMYBs with anthocyanin-promoting MYBs. Arrowheads indicate the conserved R39, V64, A90, and ANDV at positions 90 to 93 for dicot anthocyanin-promoting MYBs. Arrows indicate specific residues that contribute to a motif ((D/E)X₂(R/K)X₃LX₆LX₃R) interacting with a bHLH transcription factor in Arabidopsis (Zimmermann et al., 2004). Black circles indicate 15 PeMYBs isolated in this study.

Seamate ‘OX1313’ and *Phalaenopsis* spp. OX Red Shoe ‘OX1408’ (Supplemental Fig. S4). *PeWDR1* was chosen for its 87% identity to Arabidopsis *AtAN11*, which is responsible for anthocyanin accumulation in Arabidopsis (de Vetten et al., 1997). *PeWDR1* expressed in all three

floral organs of *P. aphrodite* ssp. *formosana* and *Phalaenopsis* spp. OX Brother Seamate ‘OX1313’ (Supplemental Fig. S2F). Together, these results showed that the expression of *PebHLH1*, *PebHLH2*, *PebHLH3*, and *PeWDR1* was not concomitant with the red color formation in these three cultivars, which suggests that bHLH transcription factors are not the limiting regulators for the anthocyanin accumulation in *Phalaenopsis* spp.

Transient Assay of Overexpression of *PeMYB2*, *PeMYB11*, and *PeMYB12*-Induced Expression of Their Downstream Genes

To identify the putative downstream genes that may be regulated by these *PeMYBs*, we identified the structural genes involved in the anthocyanin biosynthetic pathway in OrchidBase. *Flavanone 3-hydroxylase5* (*PeF3H5*), *PeDFR1*, and *Anthocyanidin synthase3* (*PeANS3*) expressed only in the red lip of *Phalaenopsis* spp. OX Brother Seamate ‘OX1313’ (Supplemental Fig. S2, A and G). In contrast, we detected no differential expression of *PeCHS*, *PeCHI*, and other candidates among various colors of flower organs (Supplemental Fig. S2, A and G). Moreover, *PeF3H5*, *PeDFR1*, and *PeANS3* were highly expressed in the red lip of *Phalaenopsis* spp. OX Brother Seamate ‘OX1313’ and all floral organs of *Phalaenopsis* spp. OX Red Shoe ‘OX1408’ by qRT-PCR assay (Fig. 3, G–I).

We wondered whether these *PeMYBs* can activate the expression of the downstream genes *PeF3H5*, *PeDFR1*, and *PeANS3* and thus, accumulate anthocyanin in *Phalaenopsis* spp. To test this, *Agrobacterium tumefaciens* containing various *PeMYBs* was infiltrated into white sepals/petals of *P. aphrodite* ssp. *formosana*. Overexpression of *PeMYB2* with or without the addition of *PebHLH1* resulted in red pigmentation (Fig. 4, B and F). However, overexpression of *PebHLH1*, *PeMYB11*, and *PeMYB12* per se did not result in any red color, which was similar to the negative control of *GUS* overexpression (Fig. 4). We found a 3.79- or 4.20-fold increase in anthocyanin content in *PeMYB2*-overexpressed flowers with or without the addition of *PebHLH1*, respectively, compared with the negative control (Fig. 4I). However, we detected low anthocyanin contents in both *PeMYB11*- and *PeMYB12*-overexpressed flowers with or without the addition of *PebHLH1*. *PeMYB12* conferred a 1.77-fold increase in anthocyanin content in the presence of *PebHLH1* (Fig. 4I), and therefore, *PeMYB12* also activated anthocyanin accumulation but to a much lower extent than *PeMYB2*.

GUS, *PebHLH1*, and *PeMYBs* were successfully expressed in individual ectopic overexpression plants (Fig. 4, J–N). *PebHLH1* expressed highly in plants with overexpression of both *PebHLH1* per se and *PeMYB2* + *PebHLH1* (Fig. 4N). The expression of *PeF3H5*, *PeDFR1*, and *PeANS3* was up-regulated highly in plants with overexpression of *PeMYB2* and *PeMYB2* + *PebHLH1* for a 98.03- to 1,527-fold increase in expression compared with the overexpressed *GUS* flower (Fig. 4, O–Q). Therefore, the red color formation was greatly up-regulated by *PeMYB2*. Interestingly, the expression of these three structural genes was also activated by *PeMYB11* with the

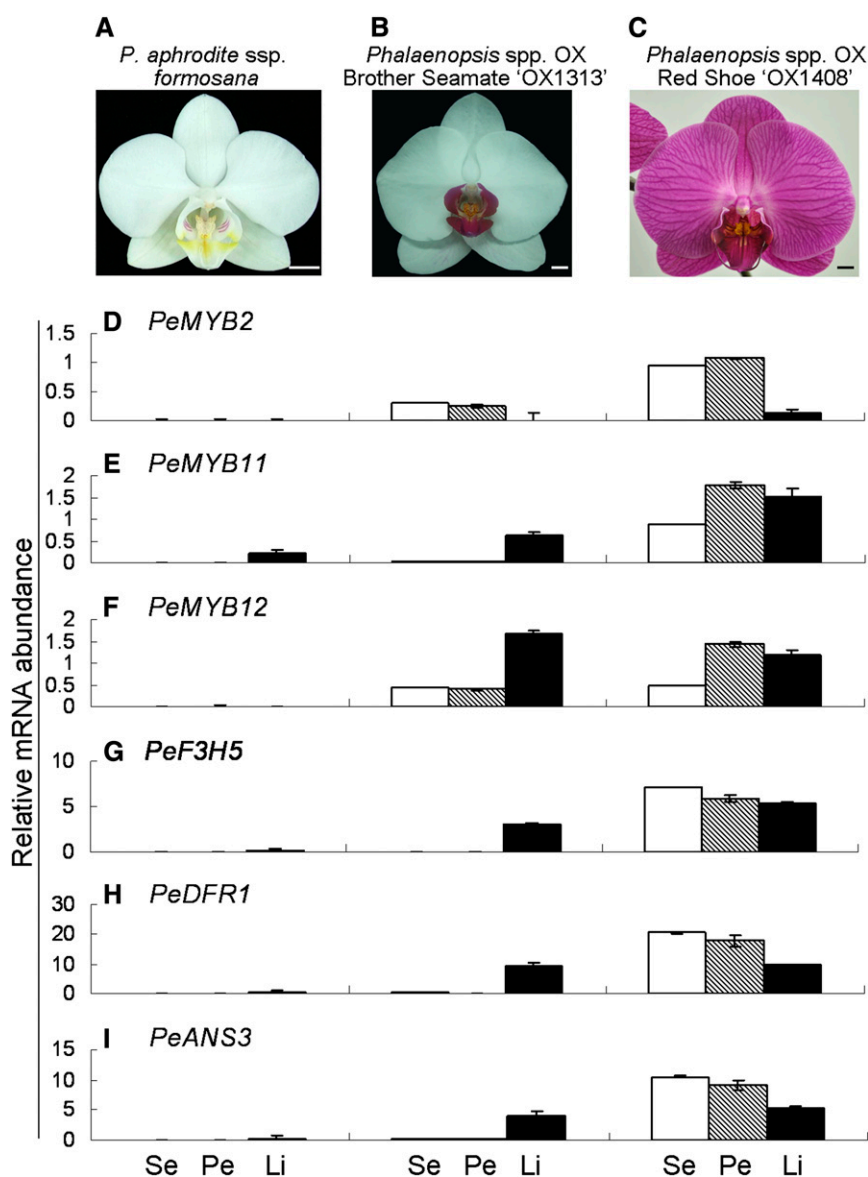


Figure 3. qRT-PCR analysis of expression profiles of the structural and regulatory genes of flower color in *P. aphrodite* ssp. *formosana* (A), *Phalaenopsis* spp. OX Brother Seamate 'OX1313' (B), and *Phalaenopsis* spp. OX Red Shoe 'OX1408' (C). The expression profiles of the regulatory genes *PeMYB2* (D), *PeMYB11* (E), and *PeMYB12* (F) and structural genes *PeF3H5* (G), *PeDFR1* (H), and *PeANS3* (I) were analyzed in sepals (Se; white bars), petals (Pe; hatched bars), and lips (Li; black bars). Data are means \pm SEM from three technological replicates and three biological samples independently and normalized to those of *PeAct4*. Bars = 1 cm.

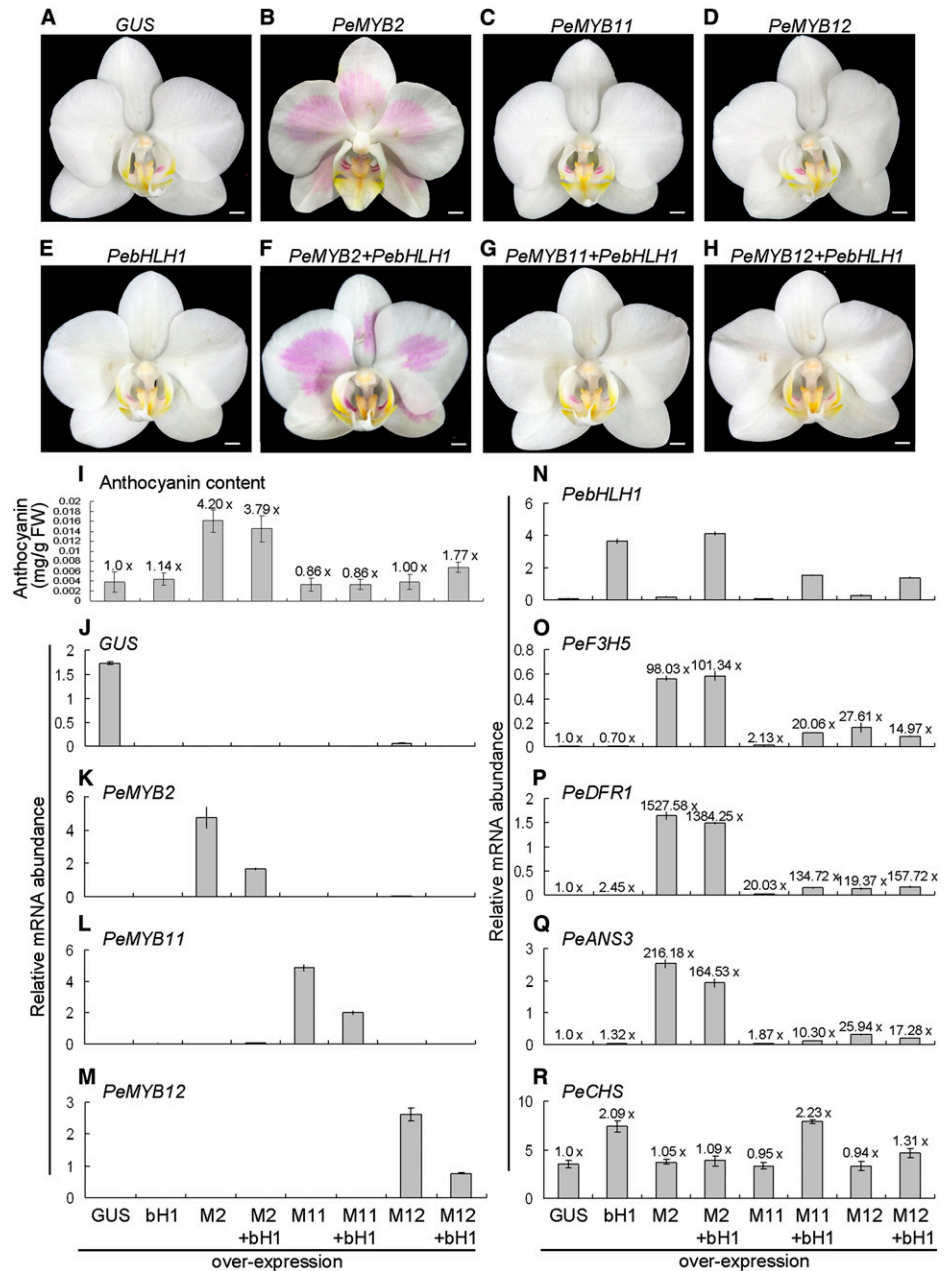
addition of *PebHLH1* and *PeMYB12* with or without the addition of *PebHLH1*, with a 10.30- to 157.72-fold increase in expression (Fig. 4, O–Q). In contrast, we detected little or no up-regulated expression of *PeF3H5*, *PeDFR1*, and *PeANS3* with *PebHLH1* overexpressed alone (Fig. 4, O–Q). *PeCHS* was constitutively expressed and showed only a 2.23-fold increase in expression with the addition of *PebHLH1* to *PeMYB11*; therefore, *PeCHS* was not regulated by these transgenes (Fig. 4R). All of these results confirmed that *PeMYB2* mainly regulated red pigmentation in *Phalaenopsis* spp. flower, and all of these *PeMYBs* could activate the expression of the late anthocyanin biosynthetic genes in *Phalaenopsis* spp. but to different levels.

Distinct Pigmentation Patterning in the Sepals/Petals within a Single Flower Regulated by Three *PeMYBs*

To further validate the in planta roles of three *PeMYBs* in regulating floral pigmentation patterning in *Phalaenopsis*

spp., we used VIGS strategy with a CymMV-based vector (Lu et al., 2012) in the red-flower *Phalaenopsis* spp. OX Red Shoe 'OX1408.' This plant was chosen, because it has various pigmentation patterning in the sepals/petals of flowers, including the full-red pigment (Fig. 5A, white arrow), venation pattern (Fig. 5A, white dashed arrow), and red spots (Fig. 5A, white arrowhead; Supplemental Fig. S5A). Intriguingly, distinct phenotypic changes on the floral pigmentation patterning resulted from silencing each individual *PeMYB*. *PeMYB2*-silenced flowers showed overall reduced pigmentation in the entire sepals but with unaffected venation pattern (Fig. 5B, black arrows). The red spots of *PeMYB11*-silenced sepals were bleached (Fig. 5C, arrowheads). *PeMYB12*-silenced sepals showed reduced venation pattern, with no effect on full-red and spot patterns (Fig. 5D, black dashed arrows). Double-silenced *PeMYB2+11* flowers showed a similar phenotype as *PeMYB2*-silenced flowers, with reduced pigment in the full-red sepals, and as *PeMYB11*-silenced but with a

Figure 4. Anthocyanin production and qRT-PCR analysis of expression profile analysis in the flowers in transient assay of overexpression of *GUS* (A), *PeMYB2* (B), *PeMYB11* (C), *PeMYB12* (D), and *PebHLH1* (E) with or without the addition of *PebHLH1* (F–H) in *P. aphrodite* ssp. *formosana* by *A. tumefaciens* infiltration. I to R, Anthocyanin contents and expression profiles in flowers with overexpression of *GUS*, *PebHLH1* (bH1), *PeMYB2* (M2), *PeMYB2* + *PebHLH1* (M2 + bH1), *PeMYB11* (M11), *PeMYB11* + *PebHLH1* (M11 + bH1), *PeMYB12* (M12), and *PeMYB12* + *PebHLH1* (M12 + bH1). The anthocyanin content and expression level detected in the negative control of overexpressed *GUS* were set to 1×, and those in the other overexpression flowers were calculated as fold change to those of the negative control as shown above each bar. This result was for three technological repeats, and the experiment was performed three times independently. FW, Fresh weight. Bars = 0.5 cm.



slight change in red spots (Fig. 5, B, C, and E). The sepals of *PeMYB11+12*-silenced flowers showed almost the same phenotype as that of *PeMYB12*-silenced flowers, with reduced venation pattern (Fig. 5, D and F). *PeMYB2+12*-silenced sepals contained bleached regions with loss of full-red and venation patterns (Fig. 5G). Because of the DNA replication competition among three viral vectors, the triple-silenced *PeMYB2+11+12* sepals showed weaker phenotype changes than single- or double-silenced sepals, with a reduced venation pattern but unaffected full-red pigmentation and red spots (Fig. 5H). Thus, *PeMYB2*, *PeMYB11*, and *PeMYB12* may participate in distinct pigmentation patterning in the sepals of a single flower: *PeMYB2* for full-red pigmentation, *PeMYB11* for red-spot formation, and *PeMYB12* for the venation pattern.

The ratios of the affected flowers to the total blossomed flowers were calculated from two independent VIGS experiments (Table I). The silencing efficiencies of single-silenced *PeMYB2*, *PeMYB11*, or *PeMYB12* were high: 63.4% to 94.7% in the sepals for each individual pigmentation pattern (Table I). Double and triple silencing of *PeMYB2* with *PeMYB11* or *PeMYB12* resulted in silencing efficiencies of 22.9% to 90.9% with reduced full-red pigmentation (Table I). Cosilencing of *PeMYB11* with *PeMYB2* showed high silencing efficiency, with bleached red spots only in experiment 1 of *PeMYB2+11*, although the silencing efficiencies of double and triple silencing of *PeMYB11* with *PeMYB2* or *PeMYB12* were very low (Table I). Moreover, the silencing efficiencies in the reduced venation pattern were

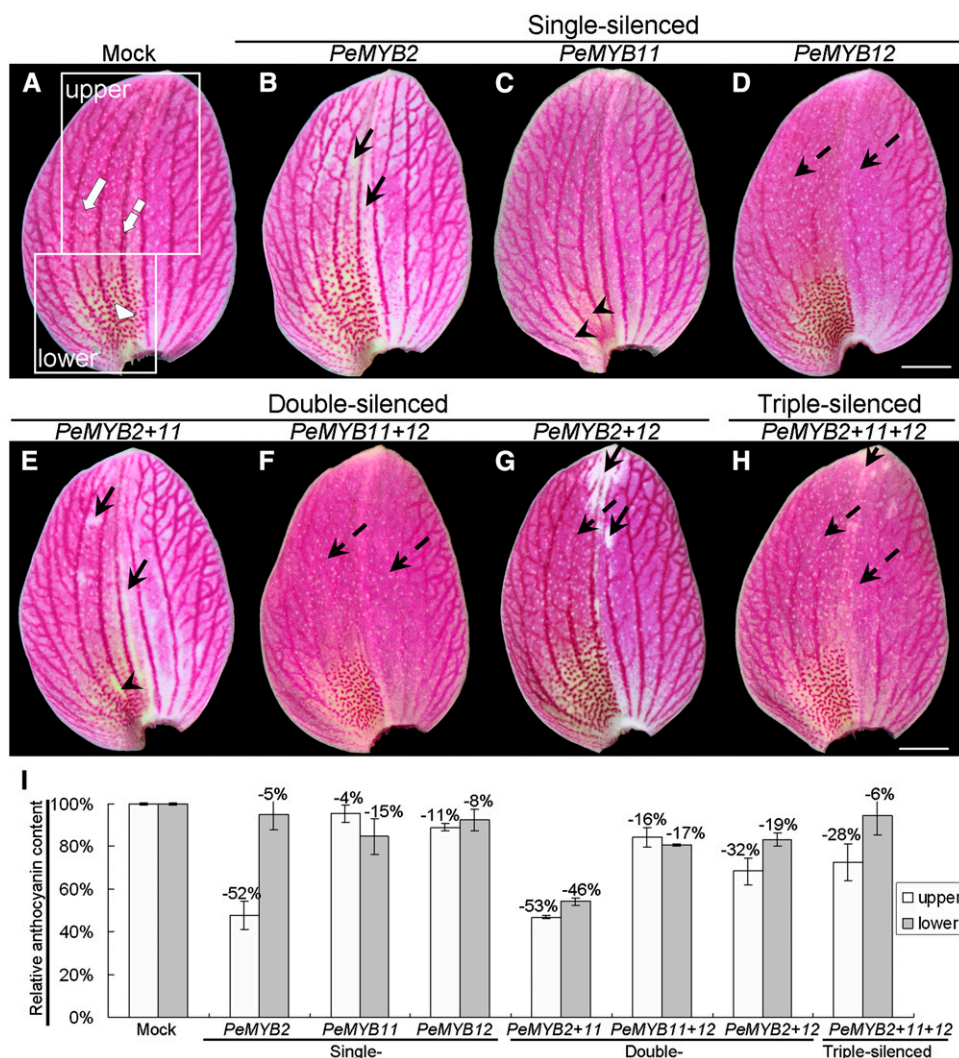


Figure 5. The sepal phenotypes of *Phalaenopsis* spp. OX Red Shoe 'OX1408' by VIGS. The adaxial surface of sepals in mock (A); single-silenced *PeMYB2* (B), *PeMYB11* (C), and *PeMYB12* (D); double-silenced *PeMYB2+11* (E), *PeMYB11+12* (F), and *PeMYB2+12* (G); and triple-silenced *PeMYB2+11+12* (H) plants. White arrow, white arrowhead, and white dashed arrow indicate full-red, red-spot, and venation patterns, respectively (A). Black arrows indicate the reduced pigmentation in whole sepals (B, E, G, and H). Black arrowheads show the absent red spots (C and E). Black dashed arrows indicate the reduced venation pigmentation (D and F–H). White boxes in A indicate the regions used to analyze anthocyanin contents of the upper (white bars) and lower (gray bars) parts of sepals (I). The anthocyanin content detected in the mock-treated sepals was set to 100%, and that in the silenced sepals was calculated as the percentage relative to that of the mock-treated sepals. Data are means \pm SEM from the first blooming flower of three plants, and they were repeated two times for VIGS experiments. Bars = 1 cm.

always high: 68.8% to 87.5% in the double and triple silencing of *PeMYB12* with *PeMYB2* or *PeMYB11* (Table I).

Anthocyanin content was measured from the upper and lower parts of the mock-treated and *PeMYB*-silenced sepals. The upper part showed the full-red color, with venation patterns at the peripheral region, and the lower part showed red spots at the base in addition to the full-red and venation patterns (Fig. 5A, boxes labeled upper and lower). *PeMYB2*-silenced sepals contained reduced anthocyanin content in the upper part, with a 52% decrease compared with that of the mock-treated sepals (Fig. 5I), which reflects *PeMYB2*'s role in full-red pigmentation in the upper part of sepals. The sepals of *PeMYB11*-silenced plants with no red spots showed a 15% decrease in anthocyanin content in the lower part, which was associated with the lack of red spots. *PeMYB12*-silenced sepals contained slightly reduced anthocyanin content in the upper and lower parts, with 11% and 8% decrease, respectively; therefore, the venation pattern extended to the lower part of sepals. Double-silenced *PeMYB2+11* sepals showed highly reduced

anthocyanin content in both upper and lower parts, with 53% and 46% decreases, respectively, in content. The double-silenced *PeMYB11+12* and *PeMYB2+12* and triple-silenced *PeMYB2+11+12* sepals showed reduced content from 6% to 32% in the upper and lower parts of sepals. Together, these results suggest that the absent pigmentation patterns in VIGS sepals resulted from the decreased anthocyanin content.

The petals of *Phalaenopsis* spp. have a similar micromorphological structure as the sepals (Hsieh et al., 2013a, 2013b; Pan et al., 2014). Similarly, the VIGS phenotypes of petals resembled those of sepals for changed pigmentation patterning on silencing of these *PeMYBs*, although much weaker (Supplemental Fig. S5).

Distinct Pigmentation Patterning in the Lip Regulated by *PeMYB11* and *PeMYB12*

Although the *Phalaenopsis* spp. lip is a modified petal, its micromorphological structure is distinct from that of petals (Hsieh et al., 2013b; Pan et al., 2014). In the VIGS experiment, only *PeMYB12*-silenced lips showed reduced

Table 1. Ratios of features of plant organs affected by *PeMYB2*, *PeMYB11*, and *PeMYB12* silencing in *Phalaenopsis* spp. OX Red Shoe ‘OX1408’

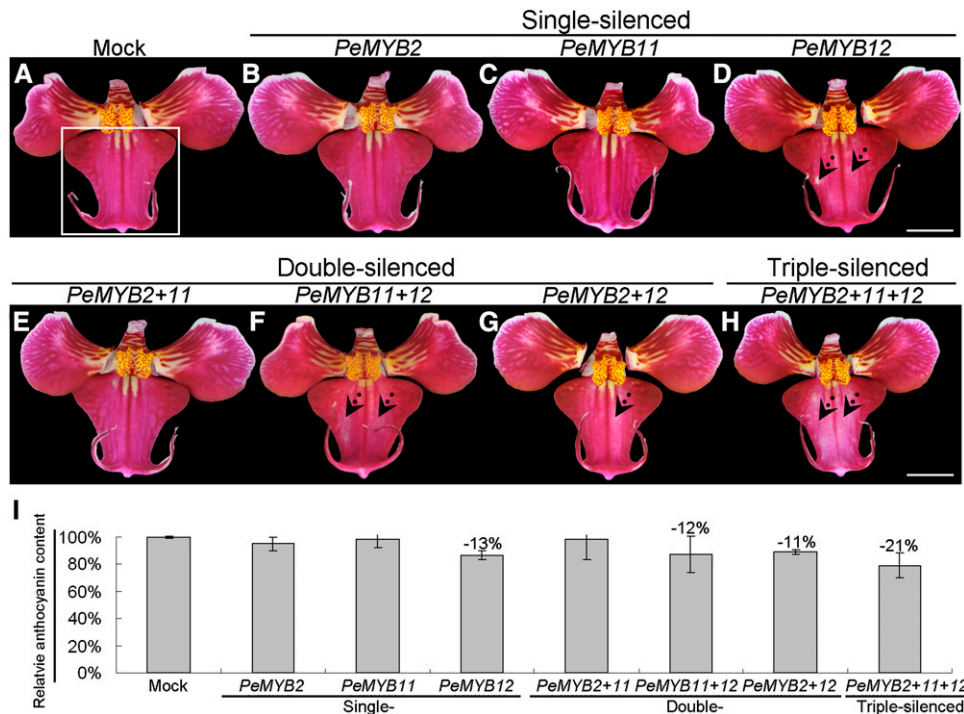
Treatments/ Replications ^a	Flowers with Color Changed						Lip
	Sepal			Petal			
	Full Red	Spot	Venation	Full Red	Spot	Venation	
<i>PeMYB2</i>							
Experiment 1	25/34 ^b (73.5) ^c	— ^d	—	21/34 (61.8)	—	—	—
Experiment 2	36/38 (94.7)	—	—	24/38 (63.2)	—	—	—
<i>PeMYB11</i>							
Experiment 1	—	33/38 (86.8)	—	—	0 ^e /38 (0)	—	—
Experiment 2	—	25/33 (75.8)	—	—	0/33 (0)	—	—
<i>PeMYB12</i>							
Experiment 1	—	—	26/41 (63.4)	—	—	25/41 (61.0)	31/41 (75.6)
Experiment 2	—	—	30/39 (76.9)	—	—	28/39 (71.8)	30/39 (76.9)
<i>PeMYB2+11</i>							
Experiment 1	30/33 (90.9)	30/33 (90.9)	—	26/33 (78.8)	0/33 (0)	—	—
Experiment 2	20/38 (52.6)	1/38 (2.6)	—	15/38 (39.5)	0/38 (0)	—	—
<i>PeMYB11+12</i>							
Experiment 1	—	1/38 (2.6)	28/38 (73.7)	—	0/38 (0)	30/38 (78.9)	26/38 (68.4)
Experiment 2	—	0/32 (0)	22/32 (68.8)	—	0/32 (0)	17/32 (53.1)	12/32 (37.5)
<i>PeMYB2+12</i>							
Experiment 1	35/39 (89.7)	—	30/39 (76.9)	21/39 (53.8)	—	25/39 (64.1)	27/39 (69.2)
Experiment 2	30/40 (75.0)	—	35/40 (87.5)	15/40 (37.5)	—	29/40 (72.5)	27/40 (67.5)
<i>PeMYB2+11+12</i>							
Experiment 1	18/36 (50.0)	0/36 (0)	28/36 (77.8)	15/36 (41.7)	0/36 (0)	27/36 (75.0)	30/36 (83.3)
Experiment 2	8/35 (22.9)	0/35 (0)	25/35 (71.4)	0/35 (0)	0/35 (0)	24/35 (68.6)	28/35 (80.0)

^aReplications of experiment per treatment. ^bNumber of affected flowers to total number of blossomed flowers in five treated plants. ^cThe ratio of affected flowers to total flowers (%). ^dThe dashes indicate that the features should not be changed by this treatment. ^eThe red spots in petal are not as obvious as in sepal.

red color in the central lobe compared with the mock-treated and single-silenced *PeMYB2* and *PeMYB11* flowers (Fig. 6, A–D). These results suggest that *PeMYB12* was the major regulator of lip pigmentation, especially for the

central lobe. The lips of double-silenced *PeMYB11+12* and *PeMYB2+12* and triple-silenced *PeMYB2+11+12* flowers showed bleached areas in the central lobe, whereas the double-silenced *PeMYB2+11* flowers did not (Fig. 6, E–H).

Figure 6. The lip phenotypes of *Phalaenopsis* spp. OX Red Shoe ‘OX1408’ by VIGS. The lips of mock (A); single-silenced *PeMYB2* (B), *PeMYB11* (C), and *PeMYB12* (D); double-silenced *PeMYB2+11* (E), *PeMYB11+12* (F), and *PeMYB2+12* (G); and triple-silenced *PeMYB2+11+12* (H) plants. Dotted arrows indicate the reduced pigmentation region in the central lobe of the lip (D and F–H). The white box in A indicates the central lobes used to analyze anthocyanin content in I. The anthocyanin content detected in the mock-treated lip was set to 100%, and that in the silenced lips was calculated as the percentage relative to that of the mock-treated lip. Data are means ± SEM from the first blooming flower of three plants, and they were repeated two times for VIGS experiments. Bars = 1 cm.



Interestingly, the bleached spots were most apparent in the triple-silenced *PeMYB2+11+12* flowers (Fig. 6H). We compared the anthocyanin content of the central lobes of lips in mock-treated (Fig. 6A, white box) and silenced plants. The lips of silenced flowers showed slightly decreased anthocyanin content (11%–21% reduction) compared with mock-treated flowers (Fig. 6I). However, because the two wings in the central lobes were not affected, they may level off the bleaching effect on anthocyanin content in these silenced plants.

We further analyzed whether these *PeMYBs* also regulated the distinct pigmentation patterning in the lip. For this, the lip of *Phalaenopsis* spp. OX Red Shoe 'OX1408' was analyzed by dissecting it into four parts, including red spots on the callus, red stripes on the lateral lobe inside, and red pigmentation on the lateral lobe outside and central lobe (Fig. 7A). The expression of *PeMYB11* was high in the callus and lateral lobe inside (Fig. 7B). This result was consistent with only *PeMYB11* expression in the red spots in the callus and lateral lobe of the lip in *P. aphrodite* ssp. *formosana* (Fig. 3; Supplemental Fig. S2B); the red stripes on the lateral lobe inside of lip of *Phalaenopsis* spp. OX Red Shoe 'OX1408' may suggest the fusion of red spots. In contrast, the expression of *PeMYB12* was high in the central lobe (Fig. 7B). Both *PeMYB11* and *PeMYB12* may participate in the distinct pigmentation patterning in the lip: *PeMYB11* for the red spots in the callus and *PeMYB12* for the red pigmentation in the central lobe of the lip.

Cytological Characterization of Various Pigmentation Patterns in the Sepals of *Phalaenopsis* spp. OX Red Shoe 'OX1408'

To study the distribution of anthocyanin production in cells with three pigmentation patterns, we analyzed cross sections of the sepal from *Phalaenopsis* spp. OX Red Shoe 'OX1408' (Fig. 8A). The full-red pigmentation showed anthocyanin concentrated in the outer layer of subepidermal cells (Fig. 8B). The red spots

showed anthocyanin accumulated in epidermal cells (Fig. 8C). The venation pattern revealed anthocyanin content in the region from subepidermal cells to the xylem (Fig. 8D). The various pigmentation patterns regulated by *PeMYB2*, *PeMYB11*, and *PeMYB12* in full-red, red-spot, and venation patterns, respectively, may result from their expression inducing anthocyanin accumulation in different cell layers of floral organs.

RNA in Situ Hybridization Reveals the Distinct Expression Profiles of *PeMYBs* Associated with Their Pigmentation Patterns

To test whether the expression of these three *PeMYBs* is associated with their distinct pigmentation patterns, we used RNA in situ hybridization. We assessed the expression profiles of all three *PeMYBs* in various floral stages and three floral organs—sepals, petals, and lip—of the red-flower *Phalaenopsis* spp. OX Red Shoe 'OX1408' (Supplemental Fig. S6, A–C). These genes showed distinct expression patterns in sepals/petals and lip. In sepals/petals, the expression of *PeMYB2* was high at stages 1 and 2 (Supplemental Fig. S6, D and E), and *PeMYB11* and *PeMYB12* were highly expressed at stage 4 (Supplemental Fig. S6, D and E). In the lip, the expression of *PeMYB11* and *PeMYB12* was high at stage 4 (Supplemental Fig. S6F), which agreed with the previous findings. *PeMYB2* was not expressed in the lip at any stages (Supplemental Fig. S6F). Therefore, we used stage 3 floral buds of *Phalaenopsis* spp. OX Red Shoe 'OX1408' for RNA in situ hybridization to further analyze the expression profiles of three *PeMYBs* and *PebHLH1*.

The expression of *PeMYB2* was detected in the subepidermal cells of both adaxial and abaxial surfaces of sepals (Fig. 9A). *PeMYB11* was detected in the cell clusters of the adaxial surface (Fig. 9D, black arrows), which reflected its red-spot pattern. *PeMYB12* was expressed in the range of cells between the xylem and epidermal cells (Fig. 9G, black arrows). Therefore, *PeMYB2*, *PeMYB11*, and *PeMYB12* showed differential expression profiles for pigmentation patterns on in situ hybridization. Moreover, the expression of *PebHLH1* was detected in subepidermal cells (Fig. 9J). As a negative control, we used hybridization with sense probes (Fig. 9, B, E, H, and K). As another negative control, the white-flower *P. aphrodite* ssp. *formosana* showed lack of expression of *PeMYB2*, *PeMYB11*, and *PeMYB12* but high expression of *PebHLH1* (Supplemental Fig. S2). RNA in situ hybridization revealed transcripts of *PebHLH1* in subepidermal cells but not *PeMYBs* (Fig. 9, C, F, I, and L).

In addition, we used RNA in situ hybridization to examine the expression of *PeMYBs* and *PebHLH1* in the lip of *Phalaenopsis* spp. OX Red Shoe 'OX1408.' *PeMYB11* was expressed in the lateral lobe and callus but not the central lobe (Fig. 10, D–F). We detected the expression of *PeMYB12* in the lateral and central lobes (Fig. 10, G–I). *PebHLH1* (Fig. 10, J–L) but not *PeMYB2* (Fig. 10, A–C) was detected in the lip. As a negative control, hybridization with the sense probe of *PeMYB12* in the lateral and central lobes and callus revealed no signals (Fig. 10,

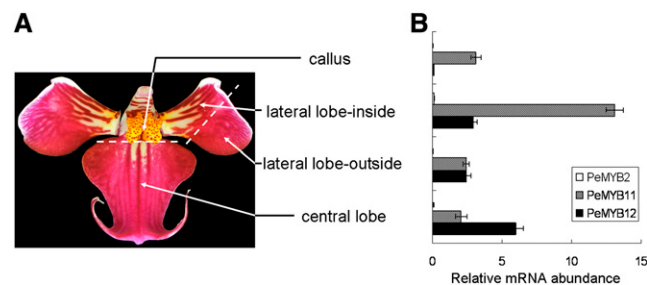


Figure 7. Expression profiles of *PeMYB11* and *PeMYB12* in the four parts of a dissected lip of *Phalaenopsis* spp. OX Red Shoe 'OX1408': callus, lateral lobe outside, lateral lobe inside, and central lobe (A). B, qRT-PCR analysis of expression profiles of *PeMYB2* (white bars), *PeMYB11* (hatched bars), and *PeMYB12* (black bars). Data are means \pm SEM from three technological replicates and three biological samples independently and normalized to that of *PeAct4*.

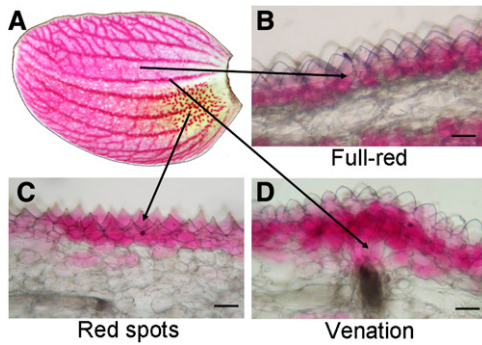


Figure 8. Cross section of the sepal of *Phalaenopsis* spp. OX Red Shoe 'OX1408' showing the distribution of anthocyanin production in full-red, red-spot, and venation patterns. The sepal phenotype (A) and the locations in cross sections of full-red (B), red-spot (C), and venation (D) patterns. Bars = 0.1 mm.

M–O). All of these results confirmed that *PeMYB11* and *PeMYB12* may participate in the distinct pigmentation patterning in the lip.

Confirmation of Distinct Expression of *PeMYBs* in Various Cultivars with Different Color Patterns

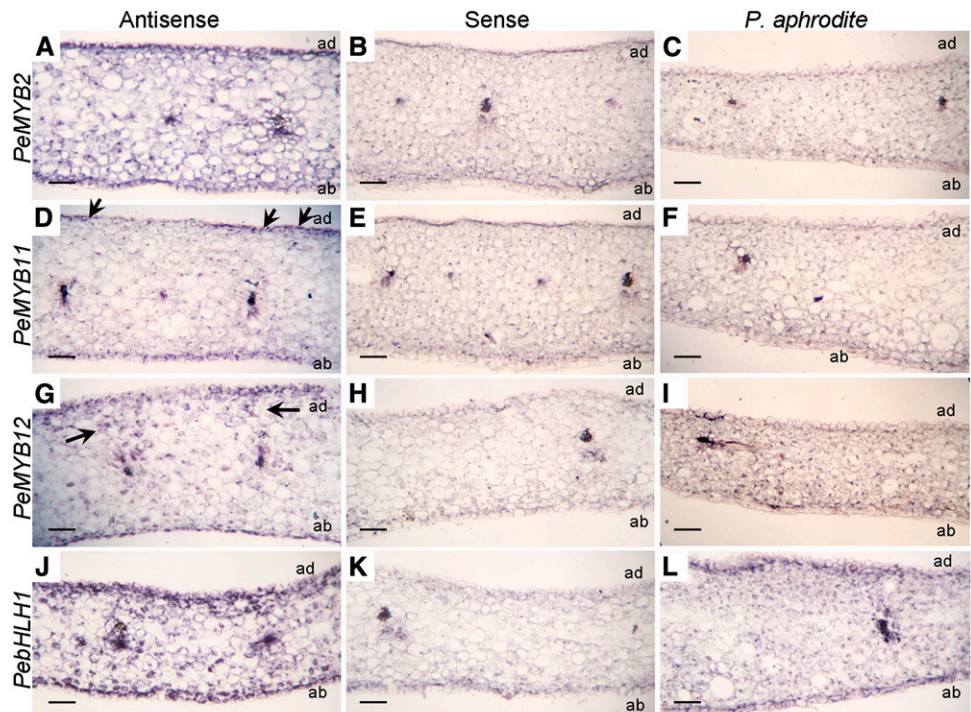
We further verified the distinct pigmentation patterning in the sepals/petals regulated by three *PeMYBs* by analyzing the expression profiles in the sepals/petals of six *Phalaenopsis* spp. cultivars with different color patterns. The flowers of *Phalaenopsis* spp. Luchia Pink 'KHM1078' and *Phalaenopsis* spp. OX Firebird 'OX1527' contain full-

red pigmentation with different intensities (Fig. 11, A and B). The expression of *PeMYB2* was high in *Phalaenopsis* spp. Luchia Pink 'KHM1078' and *Phalaenopsis* spp. OX Firebird 'OX1527' (Fig. 11, C and D) associated with their full-red pigmentation. *Phalaenopsis* spp. I-Hsin White Tiger 'KHM2215' and *Phalaenopsis* spp. I-Hsin Sesame 'OX1224' contain red spots (Fig. 11, E and F). We detected a combination of moderate to high expression of *PeMYB2* and *PeMYB11* in *Phalaenopsis* spp. I-Hsin White Tiger 'KHM2215' and *Phalaenopsis* spp. I-Hsin Sesame 'OX1224' (Fig. 11, G and H), which indicates the role of *PeMYB11* in red-spot formation. *Phalaenopsis* spp. I-Hsin Spot Leopard 'KHM1499' and *Phalaenopsis* spp. Leopard Prince 'KHM2267' contain the venation pattern with red spots on the base of the sepals (Fig. 11, I and J). We detected a combination of *PeMYB11* and *PeMYB12*, with higher expression of *PeMYB12*, associated with their major venation pattern and some red-spot formation at the base of sepals (Fig. 11, K and L). Overall, the expression profiles of *PeMYB2*, *PeMYB11*, and *PeMYB12* were concomitant with distinct floral pigmentation patterns in these six cultivars (Fig. 11). These results suggest that the combinational expression of these three *PeMYBs* contributes a wealth of natural variation in floral color patterns of *Phalaenopsis* spp. with different pigmentation intensities and patterning.

DISCUSSION

Phalaenopsis spp. are popular ornamental plants worldwide for their long-lived flowers with various flower colors and pigmentation patterning that may be linked to

Figure 9. RNA in situ hybridization analysis of *PeMYB2*, *PeMYB11*, *PeMYB12*, and *PebHLH1* transcripts in the stage 3 sepals of *Phalaenopsis* spp. Transverse sections of the sepals of *Phalaenopsis* spp. OX Red Shoe 'OX1408' were hybridized with antisense or sense RNA probes of *PeMYB2* (A and B), *PeMYB11* (D and E), *PeMYB12* (G and H), and *PebHLH1* (J and K). Transverse sections of the sepals of *P. aphrodite* ssp. *formosana* were hybridized with antisense probes of *PeMYB2* (C), *PeMYB11* (F), *PeMYB12* (I), and *PebHLH1* (L). Black arrows indicate the detected signals. ab, Abaxial surface; ad, adaxial surface. Bars = 0.1 mm.



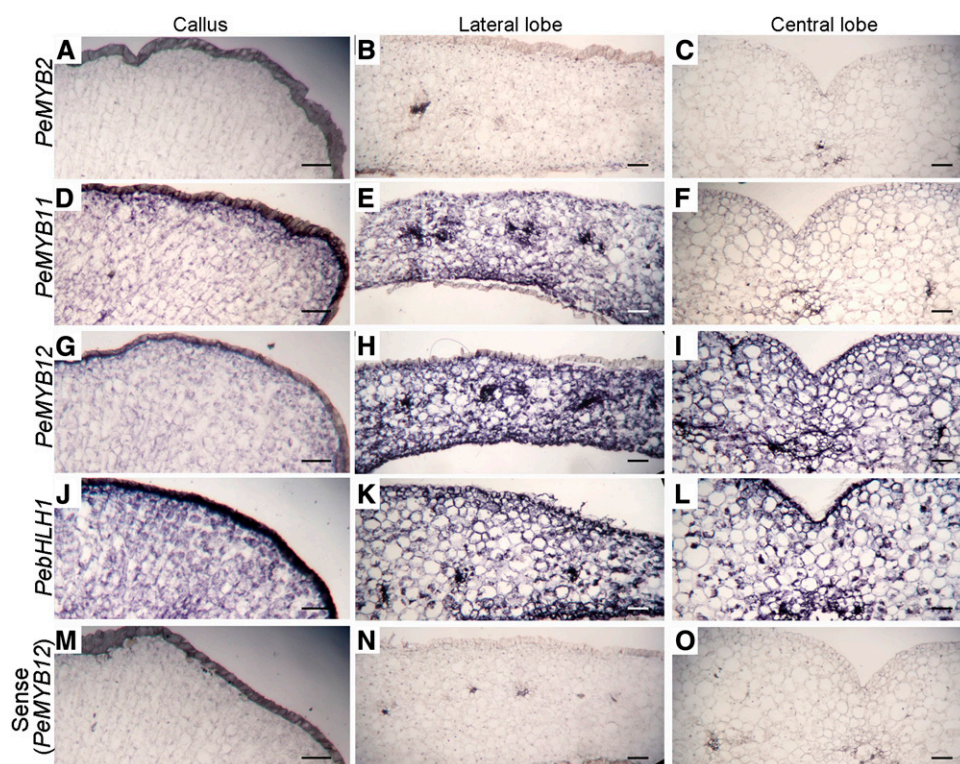


Figure 10. RNA in situ hybridization analysis of *PeMYB2*, *PeMYB11*, *PeMYB12*, and *PebHLH1* transcripts in the stage 3 lip of *Phalaenopsis* spp. OX Red Shoe 'OX1408.' Transverse sections of the lips were hybridized with antisense RNA probes of *PeMYB2* (A–C), *PeMYB11* (D–F), *PeMYB12* (G–I), and *PebHLH1* (J–L) and sense probes of *PeMYB12* (M–O) in the callus and lateral and central lobes. Bars = 0.1 mm.

their high interactions with their pollinators or artificial selection. However, the molecular mechanism of anthocyanin biosynthesis and pigmentation patterning for *Phalaenopsis* spp. flowers has not been well studied. Our results suggest that *PeMYB2*, *PeMYB11*, and *PeMYB12* activate the expression of anthocyanin biosynthetic genes *PeF3H5*, *PeDFR1*, and *PeANS3* and result in the red pigmentation in *Phalaenopsis* spp. flowers. Interestingly, *PeMYB2*, *PeMYB11*, and *PeMYB12* participated in the regulation of distinct floral pigmentation patterning, which contributed to the three differential patterns present in a single flower. In addition, different pigmentation patterns were regulated by these *PeMYBs* between the sepals/petals and lip, which suggests two sets of regulatory mechanisms related to the morphologic features of *Phalaenopsis* spp. flowers. The combined expression of different *PeMYBs* resulted in a wealth of various floral pigmentation patterning in *Phalaenopsis* spp.

Distinct Pigmentation Patterning Revealed by VIGS and RNA in Situ Hybridization Assays

The abundant *Phalaenopsis* spp. species and cultivars provide good materials for studying the regulatory mechanism of floral pigmentation patterning and other flower features (Hsiao et al., 2011). The VIGS approach with a modified CymMV-based vector was useful for screening the in planta functions of most genes for functional genomics in *Phalaenopsis* spp. (Hsieh et al., 2013b), which is of benefit for breeding these plants with long lifecycles. In this study, we used VIGS to screen the in planta functions of *PeMYBs* and verified their roles in

the distinct pigmentation patterning in *Phalaenopsis* spp. flowers by using RNA in situ hybridization assays. Although VIGS data were not perfect for revealing the real gene functions, they provided a quick approach for gene functions in nonmodel plants. However, four small defects were present for VIGS experiments in this study as well as previous studies (Hsieh et al., 2013b). First, the changed phenotype was most severe in the first four blooming flowers and became weakened with each consecutive flower. The temporal expression of genes was during floral development, and the first four blooming flowers were at the inflorescence stage, which is more sensitive to loss of function of *PeMYBs*. A similar observation was reported previously (Hsieh et al., 2013b). Second, the changes appeared only as a mosaic phenotype; therefore, only the regions along the central veins of the sepals became bleached, but the other regions were rarely affected, which suggests the route of viral spread through vascular bundles. Third, the sepals and petals of flowers were similar in morphologic aspects, but the phenotype changes were more severe in sepals than petals, despite similar gene expression in these two floral organs. Previously, silencing of a B-class MADS-box gene, *PeMADS6*, caused sepals with reduced size and leaf-like green areas along the central veins, whereas petals showed only reduced cell size (Hsieh et al., 2013a). Fourth, compared with single-silenced plants, double- and triple-silenced plants showed reduced phenotypic changes. This finding is because of the competition of viral replication as previously reported (Hsieh et al., 2013a, 2013b; Pan et al., 2014). Overall, despite the fact that the patchy nature of VIGS is not easy to overcome,

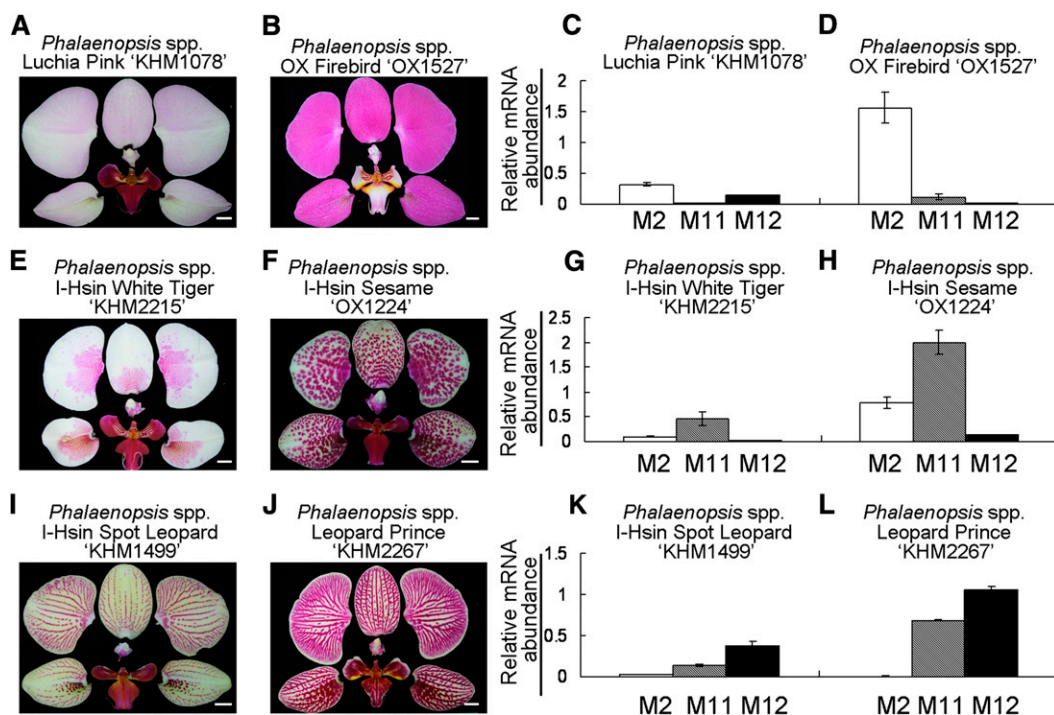


Figure 11. The expression profiles of *PeMYB2*, *PeMYB11*, and *PeMYB12* in the sepals and petals of six *Phalaenopsis* spp. cultivars with one of three pigmentation patterns. Expression of *PeMYB2* (M2; white bars), *PeMYB11* (M11; hatched bars), and *PeMYB12* (M12; black bars) was detected in *Phalaenopsis* spp. Luchia Pink 'KHM1078' (A and C), *Phalaenopsis* spp. OX Firebird 'OX1527' (B and D), *P. I-Hsin White Tiger* 'KHM2215' (E and G), *Phalaenopsis* spp. I-Hsin Sesame 'OX1224' (F and H), *Phalaenopsis* spp. I-Hsin Spot Leopard 'KHM1499' (I and K), and *Phalaenopsis* spp. Leopard Prince 'KHM2267' (J and L). Data are means \pm SEM from three technological replicates and three biological samples independently and normalized to that of *PeAct4*. Bars = 1 cm.

it is still a useful approach to study the regulation of floral pigmentation patterning, especially for plants with complicated color patterns and long lifecycles, such as *Phalaenopsis* spp.

Distinct Pigmentation Patterning Was Regulated by R2R3-MYB Transcription Factors in *Antirrhinum* spp., *Petunia* spp., and *Phalaenopsis* spp.

R2R3-MYB transcription factors play a major role in determining the pattern and intensity of floral pigmentation in *Antirrhinum* spp. and *Petunia* spp. (Schwinn et al., 2006; Albert et al., 2011). *Ros1* contributes to the strong full-red corolla pigmentation in *A. majus* (Schwinn et al., 2006). With loss of the *Ros1* function, *Ros2* affects the weak pigmentation in the inner epidermis of the corolla lobes, and *Venosa* results in the epidermal-specific venation pattern (Schwinn et al., 2006; Shang et al., 2011). *Venosa* transcript is detected in a wedge of cells between the vein and the adaxial epidermis (Shang et al., 2011). *Delila*, a bHLH factor, expresses in an epidermal-specific pattern in the corolla (Goodrich et al., 1992; Jackson, 1992), whereas the WDR protein is constitutively expressed and may move to neighboring cells (Walker et al., 1999; Bouyer et al., 2008). Thus, the epidermal-specific venation pattern in *Antirrhinum* spp. is determined by the overlap of the expression domains of the MYB and bHLH factors involved in anthocyanin production (Shang et al., 2011).

In *Petunia* spp., *AN2* controls strong, full-petal limb pigmentation, and *AN4* regulates pigments accumulated in the flower tube and anther (Quattrocchio et al., 1998, 1999). In *Petunia* spp. lines without *AN2* and *AN4* function, light-regulated pigmentation on the abaxial petal surface of flower buds (bud-blush pattern) is regulated by *PURPLE HAZE* (*PHZ*), and the venation pattern in the flower tube is controlled by *DEEP PURPLE* (*DPL*; Albert et al., 2011). All *AN2*, *AN4*, *PHZ*, and *DPL* share common bHLH (*AN1*) and WDR (*AN11*) factors (Albert et al., 2011).

In this study, we showed that three R2R3-MYB transcription factors (*PeMYB2*, *PeMYB11*, and *PeMYB12*) participated in the distinct pigmentation patterns in *Phalaenopsis* spp. flowers. These three *PeMYBs* seemed to interact with endogenous, common bHLH and WDR factors, because the expression of *PebHLH1*, *PebHLH2*, *PebHLH3*, and *PeWDR1* was either not concomitant with the red-color formation or not specific to distinct pigmentation patterns.

In addition, for both *Antirrhinum* spp. and *Petunia* spp., *Ros1* and *AN2* regulate the strong, full-red flower color, and the other pigmentation patterns only appeared when *Ros1* or *AN2* is loss of function. In contrast, in *Phalaenopsis* spp., these pigmentation patterns regulated by three *PeMYBs* were concomitantly present in one single flower of *Phalaenopsis* spp. OX Red Shoe 'OX1408.' The expression of *PeMYB2*, *PeMYB11*, and *PeMYB12* was majorly detected in accordance with their distinct pigmentation

patterns as revealed by in situ hybridization results. It is possible that these three *PeMYBs* not only regulate the main patterns but also, partially participate in the regulation of the other patterns. This possibility may explain why the boundary between each pigmentation pattern was difficult to define, such as the full-red and venation pigmentation or the venation pattern extending to the red spots at the central region of the sepals. Furthermore, the expression profiles of *PeMYBs* overlapped, such as both *PeMYB2* and *PeMYB12* expressed in the subepidermal cells above the vein. Therefore, the ratio of the expression of *PeMYB2*, *PeMYB11*, and *PeMYB12* may contribute to various pigmentation patterns appearing in one single flower.

MYB Transcription Factors Interacted with bHLH Factors for Their Functions

In Orchidaceae, *PeMYB2*, *PeMYB11*, and *PeMYB12* from *P. equestris*, *PsMYB* from purple-flower *P. schilleriana*, and *OgMYB1* from *Oncidium* spp. 'Gower Ramsey' all harbor the [D/E]Lx₂[R/K]x₃Lx₆Lx₃R motif for interacting with bHLH factors. Transient overexpression of both *PsMYB* and *OgMYB1* independently induces anthocyanin accumulation after particle bombardment, but *PsMYB* needs a bHLH transcription factor, *ZmLc*, from *Z. mays* (Ma et al., 2009) but not *OgMYB1* (Chiou and Yeh, 2008). Here, overexpression of *PeMYB2* and *PeMYB12* per se activated the expression of downstream genes either with or without the addition of *PebHLH1*, whereas *PeMYB11* required the addition of *PebHLH1* to activate downstream gene expression (Fig. 4). Because other R2R3-MYBs with this motif participate in more physiological functions, such as Arabidopsis Transparent Testa2 (Baudry et al., 2004) and Arabidopsis MYB-like2 (Sawa, 2002) for proanthocyanidin biosynthesis and trichrome development, respectively, the presence of this motif suggests that these MYBs require a bHLH partner but not is indicative of the candidate MYBs within the anthocyanin-promoting clade (Lin-Wang et al., 2010). Therefore, we think that the bHLH and WDR are required for anthocyanin biosynthesis, and these three *PeMYBs* may exert their functions with endogenous WDR and bHLH. In the case of *PeMYB2* and *PeMYB12*, they may perform their functions by interacting with an endogenous bHLH transcription factor (*PebHLH1*, *PebHLH2*, or *PebHLH3*), because these three *PebHLHs* were expressed at low level in all floral organs of *P. aphrodite* ssp. *formosana* (Supplemental Fig. S4). In contrast, *PeMYB11* may prefer interacting with *PebHLH1* because of the fact that overexpression of *PebHLH1* was required for the function of *PeMYB11*.

The Distinct Pigmentation Patterning Regulated by *PeMYB2*, *PeMYB11*, and *PeMYB12* Might Be Concomitant with the Morphological Features in *Phalaenopsis* spp.

PeMYB2 showed the remarkable high transactivational activity for anthocyanin accumulation within

transient expression assay, but interestingly, the transcript of *PeMYB2* was detected only in the sepals/petals but not lip (Fig. 3), which suggests that the regulatory strategy for anthocyanin production is coordinated with their distinct morphologic features in a single flower. Previous study showed that overexpression of a B-class *Torenia fournieri* *GLOBOSA* revealed altered cell shapes on the surfaces of sepals to a petal-like shape, and the sepals accumulated anthocyanin similar to petals of wild-type *torenia* (Sasaki et al., 2010). In *Phalaenopsis* spp., the flowers of a down-regulated B-class *PISTILLATA*-like *PeMADS6* showed discolored areas in sepals, petals, and lip (Hsieh et al., 2013a, 2013b). The link between the expression of MADS-box genes and the accumulation of anthocyanin has been reported in Arabidopsis, bilberry (*Vaccinium myrtillus*), and sweet potato (*Ipomoea batatas*; Nesi et al., 2002; Debeaujon et al., 2003; Lalusin et al., 2006; Jaakola et al., 2010). Previously, we have shown that *PeMADS2*, a B-class MADS-box gene, is strongly expressed in the sepals and petals (Tsai et al., 2004). Whether there is any correlation between *PeMADS2* and *PeMYB2* requires further study.

PeMYB11 participated in the regulation of the red spots in sepals/petals and lip of *Phalaenopsis* spp. However, red spots were absent only in the sepals/petals of single-silenced *PeMYB11* but not double- and triple-silenced *PeMYB11* or the lip of *PeMYB11*-silenced flowers. The red spots were located in the basal region of the sepals/petals and lip, and therefore, the red-spot pattern may be difficult to change during flower development. Previous study reported that the double-silenced flower of C-class *PeMADS1* and B-class *PeMADS6* showed only the margins of sepals and petals as curly and discolored (Hsieh et al., 2013b), which suggests that the margins of flowers are easier to affect by gene silencing than the basal region. Therefore, only the single-silenced *PeMYB11* sepal showed the absence of red spots but not the double- and triple-silenced sepals with decreasing silencing efficiency. Moreover, because of the location and special structure of the callus of the lip, the red spots were not affected in all VIGS flowers.

PeMYB12 participated in the regulation of different pigmentation patterns in various floral organs in a single flower: the venation pattern in the sepals/petals (Figs. 5D and 9G) but the full pigmentation pattern in the central lobe of the lip (Figs. 6D, 7, and 10I). The results of the venation pattern caused by *Venosa* and *DPL* in *Antirrhinum* spp. and *Petunia* spp., respectively, suggest a common mechanism for venation pigmentation in a wide range of plant species. Several *Phalaenopsis* spp. cultivars verified the role of *PeMYB12* in the venation pattern (Fig. 11, I–L), and confirmation is needed for whether all *Phalaenopsis* spp. cultivars with the venation pattern also contained the full pigmentation in the central lobe of lip. This differential regulatory mechanism may result from the distinct floral organs causing a diverse morphology between the sepals/petals and lip.

PeMYB2, PeMYB11, and PeMYB12 for Molecular Breeding of Cultivars with Various Color Patterns

We examined the pigmentation patterning of full-red, red-spot, and venation patterns regulated by *PeMYB2*, *PeMYB11*, and *PeMYB12*, respectively, in six *Phalaenopsis* spp. cultivars. Our findings suggest their involvement in regulating the pigmentation patterning of a single *Phalaenopsis* spp. flower and that they are required but not sufficient for deciphering the pigmentation patterning in *Phalaenopsis* spp. flowers. Thus, *PeMYB2*, *PeMYB11*, and *PeMYB12* could be molecular markers for predicting various pigmentation patterning and choosing suitable parents for molecular breeding in *Phalaenopsis* spp. A wealth of various *Phalaenopsis* spp. cultivars facilitates the study of floral pigmentation patterning, which is difficult to investigate in many other plant species.

PeMYB2 Showed High Transactivational Activity for Anthocyanin Biosynthesis

Although *PeMYB2*, *PeMYB11*, and *PeMYB12* were grouped together in the same clade in the phylogenetic analysis, *PeMYB2* showed high transactivational activity for anthocyanin biosynthesis, whereas *PeMYB11* and *PeMYB12* contained fewer activities. The amino acid sequence of *PeMYB2* showed about 80% identity and 41.9% to 43.0% identity to the MYB-R2R3 regions and the full-length complementary DNA (cDNA) of *PeMYB11* and *PeMYB12*, respectively (Supplemental Table S1). Compared with *PsMYB* and *OgMYB1*, *PeMYB11* was most similar to *PsMYB*, with 95.2% identity and 85.4% identity to the MYB-R2R3 region and the full-length cDNA, respectively (Supplemental Table S1). However, transient overexpression of *PsMYB* can induce anthocyanin accumulation after particle bombardment, but *PeMYB11* cannot. Therefore, the sequence homologies between *PeMYB2*, *PeMYB11*, *PeMYB12*, *PsMYB*, and *OgMYB1* did not directly reflect their transactivational activity for activating the anthocyanin biosynthetic pathway. Alternatively, it is possible that repressors may be present

in *P. aphrodite* ssp. *formosana* and negatively regulate the transactivational activities of *PeMYB11* and *PeMYB12*, such as R3-MYB and R2R3-MYB repressors (Albert et al., 2014).

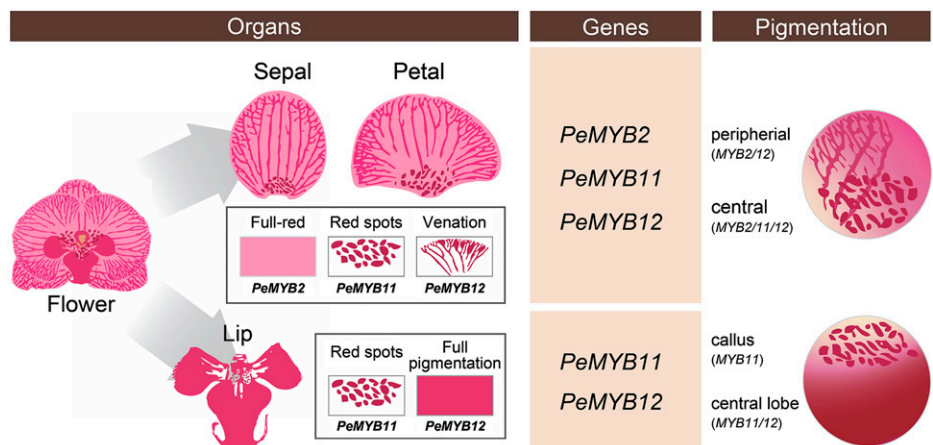
Other PeMYBs May Also Participate in Anthocyanin Accumulation in Phalaenopsis spp.

We isolated 16 R2R3-MYB transcription factors by screening OrchidBase, an Orchidaceae transcriptome database, and characterized three *PeMYBs* (*PeMYB2*, *PeMYB11*, and *PeMYB12*) in this study. For the other *PeMYBs*, *PeMYB1*, *PeMYB13*, and *PeMYB14* were grouped together and categorized into the same large clade with *PeMYB2*, *PeMYB11*, *PeMYB12*, and dicot anthocyanin-related MYBs (Fig. 1). However, we detected no expression of *PeMYB1*, *PeMYB13*, and *PeMYB14* in *P. aphrodite* ssp. *formosana* and *Phalaenopsis* spp. OX Brother Seamate ‘OX1313’ (Supplemental Fig. S2F). These three genes may express and regulate anthocyanin content in other *Phalaenopsis* spp. cultivars. In addition, *PeMYB4*, *PeMYB5*, *PeMYB6*, *PeMYB7*, and *PeMYB8* were grouped with *AtMYB4* (Jin et al., 2000), *FaMYB1* (Aharoni et al., 2001), and other MYBs that are repressors of flavonoid biosynthesis and shared the Ethylene Responsive Factor-associated amphiphilic repression repressive motif (conserved PDLNLELSIS; Aharoni et al., 2001) in their C terminus. *PeMYB4*, *PeMYB5*, *PeMYB6*, *PeMYB7*, and *PeMYB8* may exert a negative regulation on anthocyanin biosynthesis and interact with *PeMYB2*, *PeMYB11*, and *PeMYB12*.

CONCLUSION

We propose a model of three R2R3-MYB transcription factors (*PeMYB2*, *PeMYB11*, and *PeMYB12*) involved in floral anthocyanin pigmentation patterning in *Phalaenopsis* spp. (Fig. 12). In the sepals/petals, *PeMYB2*, *PeMYB11*, and *PeMYB12* regulate full-red pigmentation, red spots, and venation pattern, respectively. Moreover, the regulation of pigmentation patterning by *PeMYBs* differed in

Figure 12. Proposed model for *PeMYB2*, *PeMYB11*, and *PeMYB12* involved in anthocyanin pigmentation patterning in *Phalaenopsis* spp. flowers. In the sepals/petals, *PeMYB2*, *PeMYB11*, and *PeMYB12* regulate full-red pigmentation, red spots, and venation pattern, respectively. Moreover, *PeMYB11* controls the red spots in the callus, and *PeMYB12* regulates full pigmentation in the central lobe of the lip. The combined expression of two or three *PeMYBs* results in various pigmentation patterns in *Phalaenopsis* spp.



sepals/petals and the lip. *PeMYB11* controls the red spots in the callus, and *PeMYB12* is the major factor for pigmentation in the central lobe of the lip. We detected the combined expression of two or three *PeMYBs* resulting in various pigmentation patterns in a single flower. This study will benefit understanding of the genetic basis of the regulatory mechanism for flower color and pigmentation patterning in *Phalaenopsis* spp. and molecular breeding of *Phalaenopsis* spp. cultivars with various pigmentation patterns.

MATERIALS AND METHODS

Plant Materials

Phalaenopsis aphrodite ssp. *formosana* with white sepals/petals and a yellow lip and *Phalaenopsis* spp. OX Brother Seamate 'OX1313' with white sepals/petals and a red lip were used for identifying anthocyanin-related genes. The former was also used for transient gene overexpression analysis, because the white sepals/petals were beneficial for detecting anthocyanin accumulation. A third plant, red-flower *Phalaenopsis* spp. OX Red Shoe 'OX1408' containing various floral pigmentation patterning, was used for VIGS analysis. In addition, six *Phalaenopsis* spp. cultivars were used for verifying the regulatory roles of *PeMYBs* on the pigmentation patterning, and they included *Phalaenopsis* spp. Luchia Pink 'KHM1078', *Phalaenopsis* spp. OX Firebird 'OX1527', *Phalaenopsis* spp. I-Hsin White Tiger 'KHM2215', *Phalaenopsis* spp. I-Hsin Sesame 'OX1224', *Phalaenopsis* spp. I-Hsin Spot Leopard 'KHM1499', and *Phalaenopsis* spp. Leopard Prince 'KHM2267' (Fig. 9).

All plants were purchased from Taiwan Sugar Corp. and OX Orchid Farm and grown in the greenhouse at National Cheng Kung University under natural light and controlled temperature from 23°C to 27°C.

Identification and Phylogenetic Analysis of *PeMYBs*

The sequences of 125 R2R3-MYB transcription factors from *Arabidopsis* (*Arabidopsis thaliana*) and the anthocyanin-promoting MYBs from other plant species were used to screen the homologous genes in OrchidBase, a collection of transcriptomic sequences from *Phalaenopsis* spp. cDNA libraries (Fu et al., 2011; Tsai et al., 2013), by using a BLASTX algorithm. Moreover, the degenerated primers designed within the conserved R2R3-MYB domain were also used to amplify MYB transcription factors from the cDNA of floral buds of *P. equestris*. The R2R3 domain of MYB transcription factors was first aligned by using the default settings in ClustalW and MUSCLE implemented in MEGA version 5.2 (Tamura et al., 2011) and used to construct the phylogenetic tree with the Maximum Likelihood method. We used 1,000 bootstrapping data sets to estimate the confidence of each tree clade. Sequences of R2R3-MYBs from other plants were obtained from GenBank (<http://www.ncbi.nlm.nih.gov/>), and the accession numbers are as follows: *Antirrhinum majus* AmROS1 (ABB83826), AmROS2 (ABB83827), and AmVENOSA (ABB83828); apple (*Malus domestica*) MdMYBA (BAF80582); *Capsicum annuum* CaMYB (CAE75745); *Dendrobium* spp. DwMYB1 (AAO49410), DwMYB2 (AAO49411), DwMYB8 (AAO49417), and DwMYB10 (AAO49419); *Fragaria ananassa* FaMYB1 (AAK84064); *Gerbera hybrid* GhMYB10 (CAD87010); sweet potato (*Ipomoea batatas*) IbMYB (BAF45115); *Oncidium* spp. Gower Ramsey OgMYB1 (ABS58501); *Oryza sativa* OsMYB (CAA75509); *Petunia hybrida* PhAN2 (AAF66727); *P. schilleriana* PsMYB (ACH95792); *Solanum lycopersicum* SlMYB (AAQ55181); *Vitis vinifera* VvMYBA1 (BAD18977); and *Zea mays* ZmC1 (AAA33482) and ZmP (AAA19821). The complete R2R3 region for *PeMYB15* could not be amplified by using RACE; therefore, it was excluded from the analysis.

Isolation of Plant RNA and RT to cDNA

For RNA extraction, various floral organs, including sepals, petals, and lip, in 1- to 1.5-cm floral buds were collected. Floral organs of *Phalaenopsis* spp. OX Red Shoe 'OX1408' were divided into five stages from floral buds to blooming stage (stage 1, 0–0.5 cm; stage 2, 0.5–1 cm; stage 3, 1–2 cm; stage 4, 2–3 cm; and stage 5, blooming flower; Supplemental Fig. S5, A–C). Each sample was immersed in liquid nitrogen and stored at –80°C. Total RNA was extracted by the guanidium thiocyanate method (O'Neill et al., 1993), treated with RNase-

Free DNase I (New England Biolabs) to remove residual DNA, and reverse transcribed to cDNA by use of SuperScript III (Invitrogen).

5'- and 3'-RACE

The full-length cDNA was obtained by extending the 5' and 3' ends of cDNA with use of the SMART RACE cDNA Amplification Kit (Clontech). The full-length sequences were obtained by two rounds of PCR amplifications with primary PCR with a universal primer and the first gene-specific primer. Nested PCR involved the nested universal primer and the second gene-specific primer. The primers are in Supplemental Table S2. The PCR products were cloned into pGEM-T Easy Vector (Promega); 10 to 12 colonies were randomly selected for sequencing.

RT-PCR and qRT-PCR

Primer pairs for each gene within the gene-specific regions were designed and are in Supplemental Table S2. The PCR protocol was initial denaturation at 94°C for 5 min, 30 cycles of amplification (94°C for 30 s, 55°C for 30 s, and 72°C for 1 min), and extension at 72°C for 7 min. *PeActin9* of *P. equestris* was used as an internal control (Pan et al., 2011). The amplified products were separated on 1% (w/v) agarose gel.

For qRT-PCR, the cDNA template was mixed with 2× SYBR Green PCR Master Mix (Applied Biosystems) in an ABI Prism 7000 Sequence Detection System (Applied Biosystems). Each sample was analyzed in triplicate. Reactions involved incubation at 95°C for 10 min and thermocycling for 40 cycles (95°C for 15 s and 60°C for 1 min). After amplification, melting curve analysis was used to verify amplicon specificity and primer dimer formation. The housekeeping gene *PeActin4* (AY134752) was used for normalization (Chen et al., 2005). Data are means ± SEM calculated from three technological replicates and three biological samples independently.

Transient Assay of Overexpression of *PeMYBs* by *Agrobacterium tumefaciens* Infiltration

For transient assay, the binary vector pCambia1304 was digested with *Xba*I and *Nhe*I, filled in with the Klenow fragment (New England Biolabs), and then ligated to produce the p1304Nhx vector with a reduced vector size. *GUS*, *PebHLH1*, *PeMYB2*, *PeMYB11*, and *PeMYB12* were amplified, digested with *Xho*I, and ligated to p1304Nhx to replace the gene hygromycin phosphotransferase to produce the overexpression vectors of these genes driven by the duplicated cauliflower mosaic virus 35S promoter. The recombinant vectors were transformed into *A. tumefaciens* EHA105 by electroporation. Vector-containing *A. tumefaciens* was cultured overnight at 28°C. After centrifugation, bacterial cell pellets were resuspended by adding 500 μL of Murishige and Skoog medium containing 100 μM acetosyringone to an optical density at 600 nm of 1 and allowed to stand at room temperature for 0.5 h without shaking before infiltration. The suspensions were injected into the basal regions of the sepals/petals of flowers of *P. aphrodite* ssp. *formosana*. The *A. tumefaciens*-infiltrated plants were incubated at 25°C in an incubator with a 10-h-light/14-h-dark photoperiod for 5 d. After being photographed, the flowers were stored for RNA extraction. The transient assay was performed for five plants in each experiment and repeated for three experiments independently.

VIGS of *PeMYBs*

VIGS of *PeMYB2*, *PeMYB11*, and *PeMYB12* was performed in *Phalaenopsis* spp. OX Red Shoe 'OX1408' containing various floral pigmentation patterning as described (Hsieh et al., 2013a, 2013b). The sequences located downstream from the MYB-R2R3 region to the stop codon were selected, with 435-, 328-, and 311-bp fragments for *PeMYB2*, *PeMYB11*, and *PeMYB12*, respectively. The primers are in Supplemental Table S2. In addition to single silencing, we combined two or three vectors to perform the double silencing of *PeMYB2+11*, *PeMYB2+12*, and *PeMYB11+12* and triple silencing of *PeMYB2+11+12*. Mock-treated plants were injected with an empty plasmid of *Cymbidium* mosaic virus with a Gateway system vector as a negative control to confirm that any flower color changes were not caused by the viral infection. For each VIGS experiment, we used a B-class MADS-box gene (*PeMADS6*) as a positive control because of its silencing phenotypes, such as leaf-like characteristics and inability to fully expand (Hsieh et al., 2013a). Each treatment involved five plants and was repeated for two VIGS experiments independently.

Determination of Anthocyanin Content

Anthocyanin content was quantified as previously described (Hsieh et al., 2013a). Samples were collected from the first blooming flower of six plants that showed VIGS phenotypes for each treatment and ground in liquid nitrogen. The ground powder was extracted with methanol containing 5% (v/v) trifluoroacetic acid at 4°C for 20 h and centrifuged at 10,000g for 20 min at 4°C. The absorbance of supernatants was measured for anthocyanin content with use of a spectrophotometer at 530 nm (Agilent 8453; Agilent Technologies). The anthocyanin content was calculated as the average of three measurements from each flower, with pure anthocyanin extracted from *Phalaenopsis* spp. used as an internal standard (provided by Ping-Chung Kuo, Department of Biotechnology, National Formosa University, Yunlin, Taiwan). Relative anthocyanin content was calculated as the percentage of the anthocyanin content from silenced plants to that from mock-treated plant. Data were means \pm SEM from the first blooming flower of three plants and repeated for two VIGS experiments.

RNA in Situ Hybridization

RNA in situ hybridization was performed as previously described (Pan et al., 2011). The stage 3 floral organs of *Phalaenopsis* spp. 'OX Red Shoe' 'OX1408' were fixed in fixation buffer (4% [w/v] paraformaldehyde and 0.5% [v/v] glutaraldehyde) at 4°C for 16 to 24 h. The floral organs were dehydrated through a graded ethanol series, embedded in Histoplast, and sectioned at 10 μ m with use of a rotary microtome (MICROM, HM 310; Walldorf). Tissue sections were deparaffinized with xylene, rehydrated through an ethanol series, and pretreated with proteinase K (1 μ g mL⁻¹) in 1 \times PBS at 37°C for 30 min. Prehybridization and hybridization followed previous protocols with more stringent wash conditions: two times of 1 \times SSC at 45°C for 20 min and two times of 0.5 \times SSC at 42°C for 15 min (Tsai et al., 2005). DNA substrates containing a partial C-terminal region and the 30-untranslated region were used for riboprobe synthesis. PCR products amplified with primers are in Supplemental Table S2. Each sequence of these PCR products showed no significant similarity found against the other two *PeMYBs* by using BLAST-2 sequences. The resulting PCR fragments were used as templates for synthesis of antisense and sense riboprobes with digoxigenin (DIG)-labeled UTP-DIG (Roche Applied Science) and the T7/SP6 Riboprobe In Vitro Transcription System (Promega) following the manufacturer's instructions. The RNA in situ hybridization was performed for three hybridized samples and repeated for three experiments independently.

Sequence data from this article can be found in the GenBank/EMBL data libraries under accession numbers: *PeF3H5* (KF769464), *PeDFR1* (KF769462), *PeANS3* (KF769463), *PeMYB1* to *PeMYB16* (KF769466–KF769481), and *PebHLH1* (KF769482).

Supplemental Data

The following supplemental materials are available.

Supplemental Figure S1. Examples of *Phalaenopsis* spp. cultivars with various pigmentation patterns.

Supplemental Figure S2. Expression profiles of the structural and regulatory genes of flower color in *P. aphrodite* ssp. *formosana* and *Phalaenopsis* spp. 'OX Brother Seamate' 'OX1313.'

Supplemental Figure S3. Phylogenetic analysis of *PebHLH1*, *PebHLH2*, and *PebHLH3* with anthocyanin-related bHLH transcription factors.

Supplemental Figure S4. qRT-PCR analysis of expression profiles of the bHLH transcription factors *PebHLH1*, *PebHLH2*, and *PebHLH3* in *P. aphrodite* ssp. *formosana*, *Phalaenopsis* spp. 'OX Brother Seamate' 'OX1313,' and *Phalaenopsis* spp. 'OX Red Shoe' 'OX1408.'

Supplemental Figure S5. The petal phenotypes of plants with VIGS.

Supplemental Figure S6. qRT-PCR analysis of spatial and temporal expression of three *PeMYBs* in *Phalaenopsis* spp. 'OX Red Shoe' 'OX1408.'

Supplemental Table S1. Protein sequence identities between *PeMYB2*, *PeMYB11*, *PeMYB12*, *PsMYB*, and *OgMYB1*.

Supplemental Table S2. Primers used in this study.

ACKNOWLEDGMENTS

We thank Dr. Chi-Kuang Wen (National Key Laboratory of Plant Molecular Genetics, Institute of Plant Physiology and Ecology, Shanghai Institutes for Biological Sciences, Chinese Academy of Sciences, China), Drs. Tuan-Hua David Ho and Na-Sheng Lin (Institute of Plant and Microbial Biology, Academia Sinica, Taiwan), and Drs. Kai-Wun Yeh and Keqiang Wu (Institute of Plant Biology, National Taiwan University, Taiwan) for helpful discussion of this article; Dr. Zhao-Jun Pan (Department of Life Science, National Taiwan University) for the art work in Fig. 12; and Dr. Ming-Hsien Hsieh (Tainan District Agricultural Research and Extension Station, Council of Agriculture, Taiwan) for assistance with VIGS experiments.

Received November 29, 2014; accepted February 27, 2015; published March 4, 2015.

LITERATURE CITED

- Aharoni A, De Vos CH, Wein M, Sun Z, Greco R, Kroon A, Mol JN, O'Connell AP (2001) The strawberry FaMYB1 transcription factor suppresses anthocyanin and flavonol accumulation in transgenic tobacco. *Plant J* 28: 319–332
- Albert NW, Davies KM, Lewis DH, Zhang H, Montefiori M, Brendolise C, Boase MR, Ngo H, Jameson PE, Schwinn KE (2014) A conserved network of transcriptional activators and repressors regulates anthocyanin pigmentation in eudicots. *Plant Cell* 26: 962–980
- Albert NW, Lewis DH, Zhang H, Schwinn KE, Jameson PE, Davies KM (2011) Members of an R2R3-MYB transcription factor family in *Petunia* are developmentally and environmentally regulated to control complex floral and vegetative pigmentation patterning. *Plant J* 65: 771–784
- Baudry A, Heim MA, Dubreucq B, Caboche M, Weisshaar B, Lepiniec L (2004) TT2, TT8, and TTG1 synergistically specify the expression of BANYULS and proanthocyanidin biosynthesis in *Arabidopsis thaliana*. *Plant J* 39: 366–380
- Baumann K, Perez-Rodriguez M, Bradley D, Venail J, Bailey P, Jin H, Koes R, Roberts K, Martin C (2007) Control of cell and petal morphogenesis by R2R3 MYB transcription factors. *Development* 134: 1691–1701
- Bouyer D, Geier F, Kragler F, Schnittger A, Pesch M, Wester K, Balkunde R, Timmer J, Fleck C, Hülskamp M (2008) Two-dimensional patterning by a trapping/depletion mechanism: the role of TTG1 and GL3 in *Arabidopsis* trichome formation. *PLoS Biol* 6: e141
- Chen WH, Hsu CY, Cheng HY, Chang H, Chen HH, Ger MJ (2011) Down-regulation of putative UDP-glucose: flavonoid 3-O-glucosyltransferase gene alters flower coloring in *Phalaenopsis*. *Plant Cell Rep* 30: 1007–1017
- Chen YH, Tsai YJ, Huang JZ, Chen FC (2005) Transcription analysis of peloric mutants of *Phalaenopsis* orchids derived from tissue culture. *Cell Res* 15: 639–657
- Chiou CY, Yeh KW (2008) Differential expression of MYB gene (*OgMYB1*) determines color patterning in floral tissue of *Oncidium* Gower Ramsey. *Plant Mol Biol* 66: 379–388
- Davies KM, Albert NW, Schwinn KE (2012) From landing lights to mimicry: the molecular regulation of flower colouration and mechanisms for pigmentation patterning. *Funct Plant Biol* 39: 619–638
- de Vetten N, Quattrocchio F, Mol J, Koes R (1997) The *an11* locus controlling flower pigmentation in *petunia* encodes a novel WD-repeat protein conserved in yeast, plants, and animals. *Genes Dev* 11: 1422–1434
- Debeaujon I, Nesi N, Perez P, Devic M, Grandjean O, Caboche M, Lepiniec L (2003) Proanthocyanidin-accumulating cells in *Arabidopsis* testa: regulation of differentiation and role in seed development. *Plant Cell* 15: 2514–2531
- Feller A, Macherer K, Braun EL, Grotewold E (2011) Evolutionary and comparative analysis of MYB and bHLH plant transcription factors. *Plant J* 66: 94–116
- Fu CH, Chen YW, Hsiao YY, Pan ZJ, Liu ZJ, Huang YM, Tsai WC, Chen HH (2011) OrchidBase: a collection of sequences of the transcriptome derived from orchids. *Plant Cell Physiol* 52: 238–243
- Goodrich J, Carpenter R, Coen ES (1992) A common gene regulates pigmentation pattern in diverse plant species. *Cell* 68: 955–964
- Griesbach RJ, Beck RM, Hammond J (2007) Gene expression in the *star* mutant of *Petunia x hybrida* Vilm. *J Am Soc Hortic Sci* 132: 680–690
- Grotewold E (2006) The genetics and biochemistry of floral pigments. *Annu Rev Plant Biol* 57: 761–780
- Heuschen B, Gumbert A, Lunau K (2005) A generalised mimicry system involving angiosperm flower colour, pollen and bumblebees' innate colour preferences. *Plant Syst Evol* 252: 121–137
- Hichri I, Barrieu F, Bogs J, Kappel C, Delrot S, Lauvergeat V (2011) Recent advances in the transcriptional regulation of the flavonoid biosynthetic pathway. *J Exp Bot* 62: 2465–2483

- Hsiao YY, Pan ZJ, Hsu CC, Yang YP, Hsu YC, Chuang YC, Shih HH, Chen WH, Tsai WC, Chen HH (2011) Research on orchid biology and biotechnology. *Plant Cell Physiol* 52: 1467–1486
- Hsieh MH, Lu HC, Pan ZJ, Yeh HH, Wang SS, Chen WH, Chen HH (2013a) Optimizing virus-induced gene silencing efficiency with *Cymbidium* mosaic virus in *Phalaenopsis* flower. *Plant Sci* 201–202: 25–41
- Hsieh MH, Pan ZJ, Lai PH, Lu HC, Yeh HH, Hsu CC, Wu WL, Chung MC, Wang SS, Chen WH, et al (2013b) Virus-induced gene silencing unravels multiple transcription factors involved in floral growth and development in *Phalaenopsis* orchids. *J Exp Bot* 64: 3869–3884
- Iida S, Hoshino A, Johzuka-Hisatomi Y, Habu Y, Inagaki Y (1999) Floricultural traits and transposable elements in the Japanese and common morning glories. *Ann N Y Acad Sci* 870: 265–274
- Inagaki Y, Hisatomi Y, Suzuki T, Kasahara K, Iida S (1994) Isolation of a *Suppressor-Mutator/Enhancer*-like transposable element, *Tpn1*, from Japanese morning glory bearing variegated flowers. *Plant Cell* 6: 375–383
- Itoh Y, Higeta D, Suzuki A, Yoshida H, Ozeki Y (2002) Excision of transposable elements from the chalcone isomerase and dihydroflavonol 4-reductase genes may contribute to the variegation of the yellow-flowered carnation (*Dianthus caryophyllus*). *Plant Cell Physiol* 43: 578–585
- Jaakola L, Poole M, Jones MO, Kämäräinen-Karppinen T, Koskimäki JJ, Hohtola A, Häggman H, Fraser PD, Manning K, King GJ, et al (2010) A SQUAMOSA MADS box gene involved in the regulation of anthocyanin accumulation in bilberry fruits. *Plant Physiol* 153: 1619–1629
- Jackson D, Roberts K, Martin C (1992) Temporal and spatial control of expression of anthocyanin biosynthetic genes in developing flowers of *Antirrhinum majus*. *Plant J* 2: 425–434
- Jin H, Cominelli E, Bailey P, Parr A, Mehrrens F, Jones J, Tonelli C, Weisshaar B, Martin C (2000) Transcriptional repression by AtMYB4 controls production of UV-protecting sunscreens in Arabidopsis. *EMBO J* 19: 6150–6161
- Koes R, Verweij W, Quattrocchio F (2005) Flavonoids: a colorful model for the regulation and evolution of biochemical pathways. *Trends Plant Sci* 10: 236–242
- Koseki M, Goto K, Masuta C, Kanazawa A (2005) The star-type color pattern in *Petunia hybrida* ‘red Star’ flowers is induced by sequence-specific degradation of chalcone synthase RNA. *Plant Cell Physiol* 46: 1879–1883
- Lalusin AG, Nishita K, Kim SH, Ohta M, Fujimura T (2006) A new MADS-box gene (*lbMADS10*) from sweet potato (*Ipomoea batatas* (L.) Lam) is involved in the accumulation of anthocyanin. *Mol Genet Genomics* 275: 44–54
- Lepiniec L, Debeaujon I, Routaboul JM, Baudry A, Pourcel L, Nesi N, Caboche M (2006) Genetics and biochemistry of seed flavonoids. *Annu Rev Plant Biol* 57: 405–430
- Lin-Wang K, Bolitho K, Grafton K, Kortstee A, Karunairetnam S, McGhie TK, Espley RV, Hellens RP, Allan AC (2010) An R2R3 MYB transcription factor associated with regulation of the anthocyanin biosynthetic pathway in Rosaceae. *BMC Plant Biol* 10: 50
- Lowry DB, Sheng CC, Lasky JR, Willis JH (2012) Five anthocyanin polymorphisms are associated with an R2R3-MYB cluster in *Mimulus guttatus* (Phrymaceae). *Am J Bot* 99: 82–91
- Lu HC, Chen HH, Tsai WC, Chen WH, Su HJ, Chang DC, Yeh HH (2007) Strategies for functional validation of genes involved in reproductive stages of orchids. *Plant Physiol* 143: 558–569
- Lu HC, Hsieh MH, Chen CE, Chen HH, Wang HL, Yeh HH (2012) A high-throughput virus-induced gene-silencing vector for screening transcription factors in virus-induced plant defense response in orchid. *Mol Plant Microbe Interact* 25: 738–746
- Ludwig SR, Habera LF, Dellaporta SL, Wessler SR (1989) *Lc*, a member of the maize R gene family responsible for tissue-specific anthocyanin production, encodes a protein similar to transcriptional activators and contains the myc-homology region. *Proc Natl Acad Sci USA* 86: 7092–7096
- Lunau K, Fieselmann G, Heuschen B, van de Loo A (2006) Visual targeting of components of floral colour patterns in flower-naïve bumblebees (*Bombus terrestris*; Apidae). *Naturwissenschaften* 93: 325–328
- Ma H, Pooler M, Griesbach R (2009) Anthocyanin regulatory/structural gene expression in *Phalaenopsis*. *J Am Soc Hortic Sci* 134: 88–96
- Martins TR, Berg JJ, Blinka S, Rausher MD, Baum DA (2013) Precise spatio-temporal regulation of the anthocyanin biosynthetic pathway leads to petal spot formation in *Clarkia gracilis* (Onagraceae). *New Phytol* 197: 958–969
- Medel R, Botto-Mahan C, Kalin-Arroyo M (2003) Pollinator-mediated selection on the nectar guide phenotype in the Andean monkey flower, *Mimulus luteus*. *Ecology* 84: 1721–1732
- Nesi N, Debeaujon I, Jond C, Stewart AJ, Jenkins GI, Caboche M, Lepiniec L (2002) The TRANSPARENT TESTA16 locus encodes the ARABIDOPSIS BSISTER MADS domain protein and is required for proper development and pigmentation of the seed coat. *Plant Cell* 14: 2463–2479
- O’Neill SD, Nadeau JA, Zhang XS, Bui AQ, Halevy AH (1993) Interorgan regulation of ethylene biosynthetic genes by pollination. *Plant Cell* 5: 419–432
- Pan ZJ, Chen YY, Du JS, Chen YY, Chung MC, Tsai WC, Wang CN, Chen HH (2014) Flower development of *Phalaenopsis* orchid involves functionally divergent SEPALLATA-like genes. *New Phytol* 202: 1024–1042
- Pan ZJ, Cheng CC, Tsai WC, Chung MC, Chen WH, Hu JM, Chen HH (2011) The duplicated B-class MADS-box genes display dualistic characters in orchid floral organ identity and growth. *Plant Cell Physiol* 52: 1515–1531
- Paz-Ares J, Ghosal D, Wienand U, Peterson PA, Saedler H (1987) The regulatory *c1* locus of *Zea mays* encodes a protein with homology to *myb* proto-oncogene products and with structural similarities to transcriptional activators. *EMBO J* 6: 3553–3558
- Petroni K, Tonelli C (2011) Recent advances on the regulation of anthocyanin synthesis in reproductive organs. *Plant Sci* 181: 219–229
- Quattrocchio F, Wing J, van der Woude K, Souer E, de Vetten N, Mol J, Koes R (1999) Molecular analysis of the *anthocyanin2* gene of petunia and its role in the evolution of flower color. *Plant Cell* 11: 1433–1444
- Quattrocchio F, Wing JF, van der Woude K, Mol JN, Koes R (1998) Analysis of bHLH and MYB domain proteins: species-specific regulatory differences are caused by divergent evolution of target anthocyanin genes. *Plant J* 13: 475–488
- Saito R, Fukuta N, Ohmiya A, Itoh Y, Ozeki Y, Kuchitsu K, Nakayama M (2006) Regulation of anthocyanin biosynthesis involved in the formation of marginal picotee petals in *Petunia*. *Plant Sci* 170: 828–834
- Sasaki K, Aida R, Yamaguchi H, Shikata M, Niki T, Nishijima T, Ohtsubo N (2010) Functional divergence within class B MADS-box genes *TJGLO* and *TjDEF* in *Torenia fournieri* Lind. *Mol Genet Genomics* 284: 399–414
- Sawa S (2002) Overexpression of the AtmybL2 gene represses trichome development in Arabidopsis. *DNA Res* 9: 31–34
- Schwinn K, Venail J, Shang Y, Mackay S, Alm V, Butelli E, Oyama R, Bailey P, Davies K, Martin C (2006) A small family of MYB-regulatory genes controls floral pigmentation intensity and patterning in the genus *Antirrhinum*. *Plant Cell* 18: 831–851
- Shang Y, Venail J, Mackay S, Bailey PC, Schwinn KE, Jameson PE, Martin CR, Davies KM (2011) The molecular basis for venation patterning of pigmentation and its effect on pollinator attraction in flowers of *Antirrhinum*. *New Phytol* 189: 602–615
- Spelt C, Quattrocchio F, Mol JN, Koes R (2000) *anthocyanin1* of petunia encodes a basic helix-loop-helix protein that directly activates transcription of structural anthocyanin genes. *Plant Cell* 12: 1619–1632
- Tamura K, Peterson D, Peterson N, Stecher G, Nei M, Kumar S (2011) MEGA5: molecular evolutionary genetics analysis using maximum likelihood, evolutionary distance, and maximum parsimony methods. *Mol Biol Evol* 28: 2731–2739
- Tsai WC, Fu CH, Hsiao YY, Huang YM, Chen LJ, Wang M, Liu ZJ, Chen HH (2013) OrchidBase 2.0: comprehensive collection of Orchidaceae floral transcriptomes. *Plant Cell Physiol* 54: e7
- Tsai WC, Kuoh CS, Chuang MH, Chen WH, Chen HH (2004) Four DEF-like MADS box genes displayed distinct floral morphogenetic roles in *Phalaenopsis* orchid. *Plant Cell Physiol* 45: 831–844
- Tsai WC, Lee PF, Chen HI, Hsiao YY, Wei WJ, Pan ZJ, Chuang MH, Kuoh CS, Chen WH, Chen HH (2005) *PeMADS6*, a GLOBOSA/PISTILLATA-like gene in *Phalaenopsis equestris* involved in petaloid formation, and correlated with flower longevity and ovary development. *Plant Cell Physiol* 46: 1125–1139
- Ushimaru A, Watanabe T, Nakata K (2007) Colored floral organs influence pollinator behavior and pollen transfer in *Commelina communis* (Commelinaceae). *Am J Bot* 94: 249–258
- Walker AR, Davison PA, Bolognesi-Winfield AC, James CM, Srinivasan N, Blundell TL, Esch JJ, Marks MD, Gray JC (1999) The TRANSPARENT TESTA GLABRA1 locus, which regulates trichome differentiation and anthocyanin biosynthesis in *Arabidopsis*, encodes a WD40 repeat protein. *Plant Cell* 11: 1337–1350
- Yamagishi M, Shimoyamada Y, Nakatsuka T, Masuda K (2010) Two R2R3-MYB genes, homologs of *Petunia AN2*, regulate anthocyanin biosyntheses in flower Tepals, tepal spots and leaves of asiatic hybrid lily. *Plant Cell Physiol* 51: 463–474
- Yamagishi M, Toda S, Tadaki K (2014) The novel allele of the *LhMYB12* gene is involved in splatter-type spot formation on the flower tepals of Asiatic hybrid lilies (*Lilium* spp.). *New Phytol* 201: 1009–1020
- Zimmermann IM, Heim MA, Weisshaar B, Uhrig JF (2004) Comprehensive identification of *Arabidopsis thaliana* MYB transcription factors interacting with R/B-like BHLH proteins. *Plant J* 40: 22–34